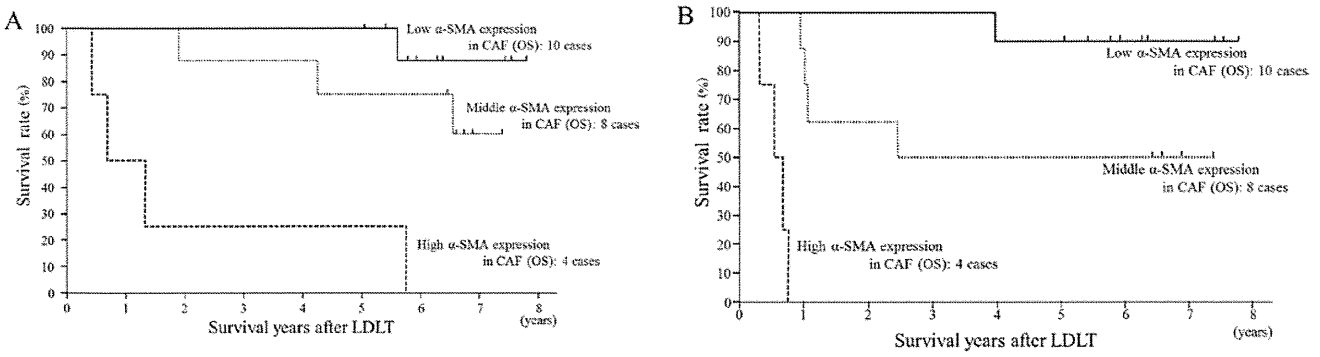

Figure 3. (A) Overall survival (OS) in living donor liver transplantation (LDLT) patients with hepatocellular carcinoma (HCC) according to proliferation of α-smooth muscle actin (α-SMA)-positive cancer-associated fibroblast (CAF) which was determined immunohistologically. Only one HCC recurrence patient died in 8 cases of low grade α-SMA-positive CAF group. All 4 cases of high grade α-SMA-positive CAF died due to HCC recurrence. The high grade α-SMA-positive CAF group had statistically significantly ($P<0.05$) poorer survival rates than the low and middle α-SMA-positive CAF groups. (B) Disease-free survival (DFS) in LDLT patients with HCC according to proliferation of α-SMA-positive CAF which was determined immunohistologically. There was only one HCC recurrence case in 8 cases of low grade α-SMA-positive CAF. All 4 cases of high grade α-SMA-positive CAF presented HCC recurrence soon after LDLT. The high grade α-SMA-positive CAF group had statistically significantly ($P<0.01$) poorer survival rates than the low and middle α-SMA-positive CAF groups, and middle grade α-SMA-positive CAF group had statistically significantly ($P<0.05$) poorer survival rates than the low grade group. There is a statistically significant correlation between post-LDLT HCC recurrence and α-SMA-positive CAF, i.e., α-SMA-positive CAF in HCC may be correlated with malignant potential of HCC progression and metastasis.

Group III (Fig. 2C), 4 cases: high grade proliferation of α-SMA-positive CAFs group; extensive proliferation of α-SMA-positive CAFs and cancer stroma accounted for >10% of ten fields under high power view.

As shown in Fig. 3, as the proliferation of α-SMA-positive CAFs increased, recurrence of HCC increased significantly, and all 4 patients in group III died soon after LDLT due to recurrence of HCC. In above Up-to-7 criteria recipients, significant proliferation of α-SMA-positive CAFs was found. In the 2 of 3 recipients who underwent HCC downstaging from above Up-to-7 to within MC by pre-LDLT therapy, recurrence of HCC was found after LDLT, and in one of these 2 cases, proliferation of α-SMA-positive CAFs was observed. On the other hand, in the one case without recurrence, proliferation of α-SMA-positive CAFs was not observed. In above Up-to-7 criteria recipients accompanied by proliferation of α-SMA-positive CAFs, the risk of HCC recurrence is very high, therefore post-operative adjuvant chemotherapy should be performed to improve survival. To improve the prognosis of recipients with HCC recurrence, appropriate anticancer therapy following recurrence is critical. We applied RFA to HCC recurrence in graft liver, and in 2 cases of recurrence with metastasis only to the lung, partial lung resection was performed. We also performed surgical resection for lymph node metastasis in the abdominal cavity. Moreover, we performed irradiation and administered molecular target drugs, and confirmed that in cases of HCC recurrence, the prognosis was improved by these intensive therapies. The proliferation of α-SMA-positive CAFs is closely related to the Up-to-7 criteria. The proliferation of α-SMA-positive CAFs, as shown in Table IV, is unrelated to pre-operative therapy or histological grade of HCC, values of tumor markers, presence of microvascular invasion, or hepatitis viruses (HBV or HCV), and appears to be a major prognostic factor in the recurrence of HCC.

From the predictors which define HCC recurrence after LT in univariate analysis, we performed a Cox-proportional multivariate analysis using three key factors such as the Up-to-7 criteria, the Tokyo criteria and proliferation of α-SMA-positive CAFs (Table V). From the results, we determined that the Up-to-7 criteria and proliferation of α-SMA-positive CAFs are both independent, most significant lyprognostic factors of LDLT for HCC.

Table V. Multivariate analysis for recipient OS using Cox's proportional hazard model of statistically more significant prognostic indicators such as Up-to-7 criteria, Tokyo criteria and α-SMA-positive CAF in hepatocellular carcinoma in univariate analysis.

Predictors	Hazard ratio	95% CI
Up-to-7 criteria[a]	61.62	2.24-1697.97
α-SMA-positive CAF[b]	8.46	1.32-54.06
Tokyo criteria[a]	0.03	0.00-1.74

[a]Criteria were evaluated by pre-operative final imaging diagnosis. [b]α-SMA-positive CAF was categorized for three grades. OS, overall survival; Up-to-7, Up-to-seven; α-SMA, α-smooth muscle actin; CAF, cancer-associated fibroblast; CI, confidence interval.

Fig. 4 shows the outcome of the present study which is the relationship between tumor number, maximum tumor diameter, microvascular invasion and proliferation of α-SMA-positive CAFs respectively for the pre-operative first imaging diagnosis prior to LDLT and pathological diagnosis. As shown in Fig. 4A based on the pre-operative first imaging diagnosis, all within Up-to-7 criteria cases survived without HCC recurrence, accounting for the largest number of cases, so these criteria appear to be the most suitable for LDLT for HCC. There were 4 cases that were diagnosed with no viable cancer lesions by pre-operative therapy for HCC such as TACL and RFA in pre-operative first imaging diagnosis, but these 4 cases had viable HCC cells. On the other hand, based on pathological diagnosis (Fig. 4B), all within Tokyo criteria recipients survived without HCC recurrence, accounting

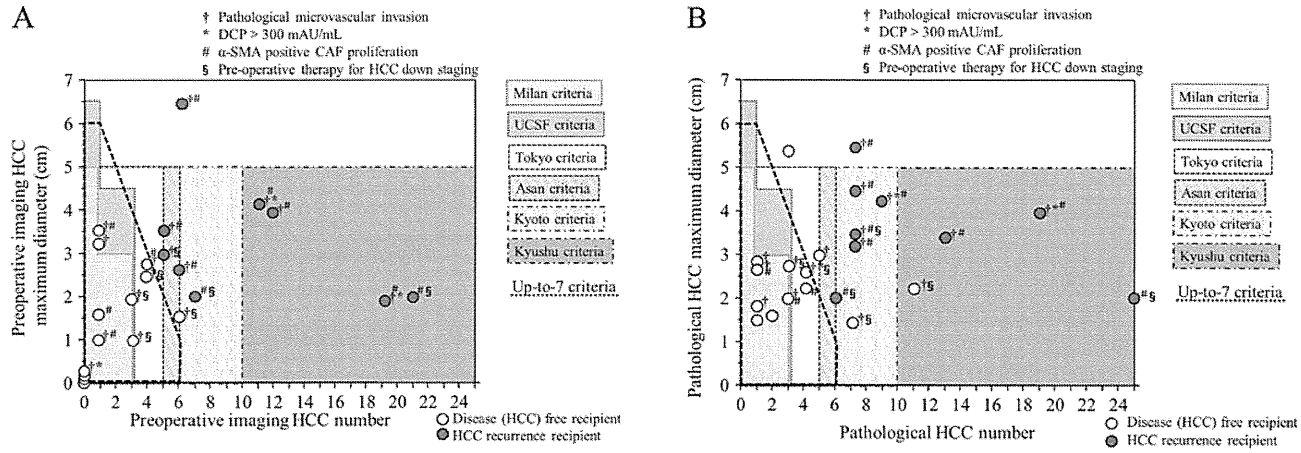

Figure 4. (A) Correlation between pre-operative imaging of hepatocellular carcinoma (HCC) maximum diameter and HCC number in living donor liver transplantation (LDLT) recipients (22 cases). This figure expresses the correlation between some eligibility criteria of liver transplantation (LT) for HCC with maximum tumor diameter, tumor number, microvascular invasion and proliferation of α-smooth muscle actin (α-SMA)-positive cancer-associated fibroblasts (CAFs). All 12 cases within Up-to-seven (Up-to-7) criteria survived without HCC recurrence. In above Up-to-7 criteria, only one case survived without HCC recurrence, and all other 9 cases presented HCC recurrence. (B) Correlation between pathological HCC maximum diameter and HCC number in LDLT recipients (22 cases). This figure expresses the correlation between some eligibility criteria of LT for HCC with maximum tumor diameter, tumor number, microvascular invasion and proliferation of α-SMA-positive CAFs. All 9 cases within Up-to-7 criteria survived without HCC recurrence. In above Up-to-7 criteria, all 4 cases that survived without HCC recurrence had no proliferation of α-SMA-positive CAF.

for the largest number of cases, so this would appear to be the most significant criteria from the viewpoint of recipient benefit. No proliferation of α-SMA-positive CAFs in HCC was found in the 4 recipients without post-LDLT HCC recurrence, who were diagnosed above Up-to-7 criteria by post-operative pathological diagnosis.

Discussion

LT continues to be associated with significant morbidity and mortality despite improvements in surgical techniques and immunosuppressive regimens. Furthermore, unlike other forms of oncological surgery, LT requires a donor organ. In view of this, utility and fairness need to be considered in relation to allocation for both donor and recipient. For this reason, the application of strict eligibility criteria such as MC has evolved as an important aspect of current clinical practice. In Japan, whether or not pre-transplant therapy is performed for HCC at 3 months prior to LT, within MC, is an essential requirement for receiving DDLT, and is also an essential requirement for receiving LDLT under the health insurance. In LDLT, since a healthy donor takes a major risk, HCC recurrence must be avoided after LT in recipients. As there is no absolute curative treatment for HCC recurrence, LDLT should be performed while adhering to strict eligibility criteria so that HCC does not recur after LT. In the present study, the OS and DFS after LDLT in patients who met Up-to-7 criteria in both pre-operative evaluation and pathological evaluation were 100% although including recurrence of HCV hepatitis, we support that Up-to-7 criteria are well-established tools for assessing the prognosis of HCC. In the pre-operative first imaging diagnosis and pathological diagnosis, there were no cases which were above MC and within UCSF criteria; however, there were 2 cases which were above MC and within Up-to-7 criteria. Therefore, we did not compare Up-to-7 criteria exceeding MC and UCSF criteria but, as shown in Fig. 4, the Up-to-7 criteria broadly cover the UCSF criteria. Moreover, in view of the fact that the only patient who survived without HCC recurrence above Up-to-7 criteria was also close to within criteria, it seems most appropriate to take the Up-to-7 criteria as suitable global standard criteria for LT in HCC.

Some of the published criteria of LT for HCC do not affect the OS after LT and appear to underestimate the risk of HCC recurrence. The reason for this may be that benign/malignant borderline lesions, such as high-grade degenerative nodules (17,23-25), are counted as HCC. High-grade degenerative nodules must be clearly distinguished from HCC and a consensus has already been reached regarding this difference (17,25). If high-grade degenerative nodules are included in HCC, it detracts from the reliability of the criteria itself. Pathologically, the ideal criteria are the Tokyo criteria, but 2 cases of recurrence were found in pre-operative first imaging diagnosis, and it is difficult to conclude that Tokyo criteria would have better eligibility criteria than the Up-to-7 criteria.

Downstaging. The downstaging refers specifically to treatment undertaken to convert a tumor with morphology beyond established LT criteria (and therefore not a candidate for LT) to a size that is within criteria and therefore enable a patient to become an LT candidate. Any assessment of the efficacy of a downstaging protocol needs not only a clear definition of which patients would be considered for downstaging, but also a clear definition of eligibility criteria that need to be met for the patient to qualify for LT. Furthermore, some protocols require a period of stability once LT criteria have been met prior to activation on waiting. Such a restriction should ensure that patients with tumors that exhibit unfavorable biology, which would be expected to translate into an increased risk of recurrence, are excluded. However, comparable post-LT outcomes in recipients who had been successfully downstaged

to recipients within MC (26-28) have been demonstrated. In the present study, we performed pre-LT therapy for downstaging in 7 recipients. Pre-LT therapy consisted of 5 cases in which only TACL was performed, and 2 cases in which RFA was performed in addition to TACL. In both situations, LDLT was performed at 3 months or more after pre-LT therapy. Four of the 5 recipients above Up-to-7 criteria who underwent pre-LT therapy were judged to be within Up-to-7 criteria from above Up-to-7 criteria in the pre-operative final diagnosis, but in the pathological diagnosis, all of these cases were judged to be above Up-to-7 criteria (allowing microvascular invasion). The reasons for the discrepancy between the pre-operative final imaging diagnosis and the pathological diagnosis are that minute, residual viable cancer lesions of TACL therapy were not identified in the images, and small HCC was judged as high-grade degenerative nodules in the pre-operative diagnosis.

α-SMA-positive CAF (myofibroblastic CAF). Lysophostatidic acid (LPA) accelerates HCC progression by recruiting peritumoral tissue fibroblasts (PTFs) and promoting their transdifferentiation into myofibroblasts (18). Following transdifferentiation, pretumoral tissue fibroblast expressed α-SMA and enhanced proliferation, migration and invasion of HCC cells occur. In the present study, proliferation of α-SMA-positive CAFs in HCC was significantly correlated with metastasis of HCC and above Up-to-7 criteria, and was therefore significantly considered a poorer prognosis factor equivalent to Up-to-7 criteria in post-LDLT recipients with HCC. It is generally accepted that HCC originates from hepatocytes but grows and advances while fully embedded in a surrounding microenvironment with a rich content of myofibroblasts, fibroblasts, and other cell types due to the underlying cirrhosis. Liver myofibroblasts, derived from quiescent fibroblasts and hepatic stellate cells activated by the chronic injury, can be recognized by their expression of α-SMA (29,30). Myofibroblasts have been detected at the advanced edge of several different malignancies as the predominant phenotype in the CAF population (31). Although the origin of CAF remains controversial, their immunophenotypical characterization, which primarily includes α-SMA and excludes epithelial and endothelial common markers, is widely accepted (29,32,33). CAFs differ from PTFs not in terms of somatic mutations but, rather, in terms of molecular and functional differences in modulating neighboring cancer cells (34,35). However, the paracrine crosstalk between HCC and stromal fibroblasts such as CAF or pretumoral tissue fibroblast is poorly understood. Stromal myofibroblasts in HCC and matching peritumoral tissues is detected by staining with anti-α-SMA antibody (29). It was found that α-SMA-positive cells were mainly expressed within the tumor stroma (18).

We also performed an immunohistochemical study for biological markers of epithelial mesenchymal transitions (EMT) in HCC which are thought to be related to cancer invasion and metastasis (36,37) (data not shown). It is reported that downregulation of E-cadherin (36-39), weakened expression (39) or overexpression of N-cadherin (40), overexpression of β-catenin (36-38), overexpression of vimentin (41,42), overexpression of Snail (36,43), overexpression of Slug (36) and overexpression of TWIST (36,39) are poor prognosis factors for HCC. We performed immunohistochemical study of these markers. The recipients with overexpression of vimentin or Snail had significantly higher risk of HCC recurrence after LT, but it did not have as much of an impact as expression of α-SMA-positive CAFs by α-SMA immunostaining. Also, when we performed a multivariate analysis using Cox's proportional method with Up-to-7 criteria or α-SMA-positive CAFs, and other histological factors in HCC, a clear correlation was found for Up-to-7 criteria and proliferation of α-SMA-positive CAFs. It was determined that these two factors alone were independent factors that specified prognosis or DFS after LDLT (Table V). In other words, proliferation of α-SMA-positive CAFs leads to a high risk of HCC metastasis and the prognosis is extremely poor even if LT is performed.

Microvascular invasion of HCC. The investigated cases in the present study did not include any cases of macrovascular invasion, and since it is reported that macrovascular invasion is a significant risk factor for recurrence of HCC (2,44-46), there is no indication of LT. On the other hand, as regards microvascular invasion, it has been reported to worsen prognosis after LT for HCC (47) and there is a conflicting report that it has no effect on the prognosis (44). If we limit the discussion to within Up-to-7 criteria, it has also been reported that the presence of microvascular invasion does not define the prognosis after LT for HCC (48). As regards the MC and Up-to-7 criteria, microvascular invasion is regarded as a factor of above criteria but, in this study, microvascular invasion did not contribute to HCC recurrence after LDLT. It is more difficult to determine the presence of microvascular invasion from pre-operative imaging (49-51), and we consider microvascular invasion should be included in the within eligibility criteria of LT for HCC. The histological type such as the combined HCC type or the poorly differentiated HCC type, and the presence of intrahepatic metastasis did not contribute to HCC recurrence after LDLT.

Pre-operative imaging diagnosis. One common methodological flaw in studies identifying clinical predictors of favorable outcome is the use of explant pathology to provide information on tumor maximum diameter and number, with the derived criteria being subsequently applied to radiological assessments of tumor burden. However, radiological staging can be limited in accuracy; indeed, review of the Eurotransplant Allocation System demonstrated a 34% accuracy of radiology in comparison to explant pathology, with tumor absent in 8.3% of patients, overstaging of the tumor in 36.2% and understaging in 10.4% (52). This is clinically significant as radiological understaging translates into inferior outcomes (53). If the precision of HCC imaging diagnosis is low, the reliability of the criteria decreases, so pre-operative imaging diagnosis must be performed accurately using multiple modalities. In order to enhance imaging diagnostic ability in HCC, the authors, in addition to dynamic MDCT and Gd-EOB-DTPA-MRI (12,13), also perform CT with angiography (CTAP and CTHA) as far as possible (14-17). We believe that by combining these tools, the ability to diagnose HCC can be enhanced to the maximum level. By performing these three tools of pre-operative imaging, the ability to diagnose benign/malignant borderline lesions and local recurrence foci after RFA or TACL therapy is also enhanced, which

made it possible to obtain a pre-operative imaging diagnosis close to a pathological diagnosis. In practice, comparing the pre-operative first diagnosis and pathological diagnosis, the sensitivity of the within Up-to-7 criteria was 100%, and the specificity was 75% which is a satisfactory result. The Up-to-7 criteria which specify eligibility for LT in HCC were found to be the criteria which clearly define prognosis in the diagnostic results obtained using these three imaging diagnostic modalities. At present, in Japan, in order to receive LDLT under health insurance, the history of therapy for HCC 3 months prior to LT is not a limitation, but satisfaction of the within MC in the pre-operative final imaging diagnosis is a requirement. However, it appears there is a sufficient scientific foundation for extending this eligibility to within Up-to-7 criteria from MC.

LDLT vs. DDLT. In general, it is said that separate consideration for LDLT for HCC is required, as the patient already has an allocated liver graft and is therefore not dependent on the donor pool. It can therefore be argued that the application of strict eligibility criteria as required with cadaveric grafts for patients with HCC is not necessary. However, in these circumstances, the risk to the donor must be incorporated into any decision, since it is clearly unethical to expose a donor to a significant risk of morbidity or mortality. Therefore, we must consider that similar criteria would apply to patients undergoing DDLT and LDLT. In fact, similar outcomes are observed in patients receiving DDLT or LDLT for HCC within Up-to-7 criteria (47). In several countries where DDLT is mainly performed for LT, the Up-to-7 criteria are accepted as the appropriate criteria (2,10,47,48,54) and it is also clear from our present study that, similarly, there must be appropriate criteria in the LDLT (48). In other words, eligibility for LT in HCC should be within the Up-to-7 criteria regardless of whether it is DDLT or LDLT.

In conclusion, the ideal eligibility criteria of LDLT for HCC is the Up-to-7 criteria and although there were some recipients in HCV hepatitis recurrence, all recipients within the criteria survived without HCC recurrence. Also, in above Up-to-7 criteria, proliferation of α-SMA-positive CAFs was found more frequently than within criteria, and this appeared to be a major factor in recurrence of HCC after LT. On the other hand, no significant correlation was found between pre-transplant treatment for HCC, histological differentiation and tumor markers with recurrence of HCC after LDLT. At present, while there is still no effective treatment for recurrence of HCC after LT and also from the viewpoint of proliferation of α-SMA-positive CAF, LT, in particular LDLT, should be limited to recipients who are within Up-to-7 criteria in pre-operative imaging diagnosis.

References

1. Mazzaferro V, Regalia E, Doci R, *et al*: Liver transplantation for the treatment of small hepatocellular carcinoma in patients with cirrhosis. N Engl J Med 334: 693-699, 1996.
2. Lee SG, Hwang S, Moon DB, *et al*: Expanded indication criteria of living donor liver transplantation for hepatocellular carcinoma at one large-volume center. Liver Tansp 114: 935-945, 2008.
3. Sugawara Y, Tamura S and Makuuchi M: Living donor liver transplantation for hepatocellular carcinoma: Tokyo University series. Dig Dis 25: 310-312, 2007.
4. Ito T, Takada Y, Ueda M, *et al*: Expansion of selection criteria for patients with hepatocellular carcinoma in living donor liver transplantation. Liver Transpl 13: 1637-1644, 2007.
5. Takada Y, Ito T, Ueda M, *et al*: Living donor liver transplantation for patients with HCC exceeding the Milan criteria: a proposal of expanded criteria. Dig Dis 25: 299-302, 2007.
6. Soejima Y, Taketomi A, Yoshizumi T, *et al*: Extended indication for living donor liver transplantation in patients with hepatocellular carcinoma. Transplantation 83: 893-899, 2007.
7. Taketomi A, Sanefuji K, Soejima Y, *et al*: Impact of des-gamma-carboxy prothrombin and tumor size on the recurrence of hepatocellular carcinoma after living donor liver transplantation. Transplantation 87: 531-537, 2009.
8. Shirabe K, Taketomi A, Morita K, *et al*: Comparative evaluation of expanded criteria for patients with hepatocellular carcinoma beyond the Milan criteria undergoing living-related donor liver transplantation. Clin Transplant 25: E491-E498, 2011.
9. Furukawa H, Shimamura T, Suzuki T, *et al*: Liver transplantation for hepatocellular carcinoma: the Japanese experience. J Hepatobiliary Pancreat Surg 17: 533-538, 2010.
10. Mazzaferro V, Llovet JM, Miceli R, *et al*: Predicting survival after liver transplantation in patients with hepatocellular carcinoma beyond the Milan criteria: a retrospective, exploratory analysis. Lancet Oncol 10: 35-43, 2009.
11. Yao FY, Ferrell L, Bass NM, *et al*: Liver transplantation for hepatocellular carcinoma: expansion of the tumor size limits does not adversely impact survival. Hepatology 33: 1394-1403, 2001.
12. Kobayashi S, Matsui O, Gabata T, *et al*: Gadolinium ethoxybenzyl diethylenetriamine pentaacetic acid-enhanced magnetic resonance imaging findings of borderline lesions at high risk for progression to hypervascular classic hepatocellular carcinoma. J Comput Asist Tomogr 35: 181-186, 2011.
13. Kobayashi S, Matsui O, Gabata T, *et al*: Intranodular signal intensity analysis of hypovascular high-risk borderline lesions of HCC that illustrate multi-step hepatocarcinogenesis within the nodule on Gd-EOB-DTPA-enhanced MRI. Eur J Radiol 81: 3839-3845, 2012.
14. Miyayama S, Matsui O, Yamashiro M, *et al*: Detection of hepatocellular carcinoma by CT during arterial portography using a cone-beam CT technology: comparison with conventional CTAP. Abdom Imaging 34: 502-506, 2009.
15. Kitao A, Zen Y, Matsui O, Gabata T and Nakanuma Y: Hepatocarcinogenesis: multistep changes of drainage vessels at CT during arterial portography and hepatic arteriography - radiologic-pathologic correlation. Radiology 252: 605-614, 2009.
16. Miyayama S, Yamashiro M, Okuda M, *et al*: Detection of corona enhancement of hypervascular hepatocellular carcinoma by C-arm dual-phase cone-beam CT during hepatic arteriography. Cardiovasc Intervent Radiol 34: 81-86, 2011.
17. Matsui O, Kobayashi S, Sanada J, *et al*: Hepatocelluar nodules in liver cirrhosis: hemodynamic evaluation (angiography-assisted CT) with special reference to multi-step hepatocarcinogenesis. Abdom Imaging 36: 264-272, 2011.
18. Mazzocca A, Dituri F, Lupo L, Quaranta M, Antonaci S and Giannelli G: Tumor-secreted lysophostatidic acid accelerates hepatocellular carcinoma progression by promoting differentiation of peritumoral fibroblasts in myofibroblasts. Hepatology 54: 920-930, 2011.
19. Okabe H, Beppu T, Hayashi H, *et al*: Hepatic stellate cells may relate to progression of intrahepatic cholangiocarcinoma. Ann Surg Oncol 16: 2555-2564, 2009.
20. Greene FL, Page DL, Fleming ID, *et al* (eds): AJCC Cancer Staging Manual. 6th edition. Springer-Verlag, New York, pp435, 2002.
21. United Network for Organ Sharing: Policy 3.6. www.unos.org. Accessed September 8, 2002.
22. Urata K, Kawasaki S, Matsunami H, *et al*: Calculation of child and adult standard liver volume for liver transplantation. Hepatology 21: 1317-1321, 1995.
23. Authors not listed: Terminology of nodular hepatocellular lesions. International Working Party. Hepatology 22: 101-105, 1995.
24. Hirohashi S, Ishak KG, Kojiro M, *et al*: Hepatocellular carcinoma. In: Pathology and Genetics of Tumours of the Digestive System. Hamilton SR and Aaltonen LA (eds). IARC Press, Lyon, pp159-172, 2000.
25. Hayashi M, Matsui O, Ueda K, *et al*: Correlation between the blood supply and grade of malignancy of hepatocellular nodules associated with liver cirrhosis: evaluation by CT during intraarterial injection of contrast medium. AJR Am J Roentgenol 172: 969-976, 1999.

26. Chapman WC, Majella Doyle MB, Stuart JE, *et al*: Outcomes of neoadjuvant transarterial chemoembolization to downstage hepatocellular carcinoma before liver transplantation. Ann Surg 248: 617-625, 2008.
27. Ravaioli M, Grazi GL, Piscaglia F, *et al*: Liver transplantation for hepatocellular carcinoma: results of down-staging in patients initially outside the Milan selection criteria. Am J Transplant 8: 2547-2557, 2008.
28. Yao FY, Kerlan RK Jr, Hirose R, *et al*: Excellent outcome following down-staging of hepatocellular carcinoma prior to liver transplantation: an intention-to-treat analysis. Hepatology 48: 819-827, 2008.
29. Serini G and Gabbiani G: Mechanisms of myofibroblast activity and phenotypic modulation. Exp Cell Res 250: 273-283, 1999.
30. Tomasek JJ, Gabbiani G, Hinz B, Chaponnier C and Brown RA: Myofibroblasts and mechano-regulation of connective tissue remodelling. Nat Rev Mol Cell Biol 3: 349-363, 2002.
31. Sappino AP, Skalli O, Jackson B, Schürch W and Gabbiani G: Smooth muscle differentiation in stromal cells of malignant and non-malignant breast tissues. Int J Cancer 41: 707-712, 1988.
32. Di Tommaso L, Pasquinelli G and Damiani S: Smooth muscle cell differentiation in mammary stromo-epithelial lesions with evidence of a dual origin: stromal myofibroblasts and myoepithelial cells. Histopathology 42: 448-456, 2003.
33. Orimo A, Gupta PB, Sgroi DC, *et al*: Stromal fibroblasts present in invasive human breast carcinomas promote tumor growth and angiogenesis through elevated SDF-1/CXCL12 secretion. Cell 121: 335-348, 2005.
34. Qiu W, Hu M, Sridhar A, *et al*: No evidence of clonal somatic genetic alterations in cancer-associated fibroblasts from human breast and ovarian carcinomas. Nat Genet 40: 650-655, 2008.
35. Haviv I, Polyak K, Qiu W, Hu M and Campbell I: Origin of carcinoma associated fibroblasts. Cell Cycle 8: 589-595, 2009.
36. Yang MH, Chen CL, Chau GY, Chiou SH, Su CW, Chou TY, *et al*: Comprehensive analysis of the independent effect of twist and snail in promoting metastasis of hepatocellular carcinoma. Hepatology 50: 1464-1474, 2009.
37. Guo C, Liu QG, Yang W, Zhang ZL and Yao YM: Relation among p130Cas, E-cadherin and beta-catenin expression, clinicopathologic significance and prognosis in human hepatocellular carcinoma. Hepatobiliary Pancreat Dis Int 7: 490-496, 2008.
38. Korita PV, Wakai T, Shirai Y, *et al*: Overexpression of osteopontin independently correlates with vascular invasion and poor prognosis in patients with hepatocellular carcinoma. Hum Pathol 39: 1777-1783, 2008.
39. Zhan DQ, Wei S, Liu C, *et al*: Reduced N-cadherin expression is associated with metastatic potential and poor surgical outcomes of hepatocellular carcinoma. J Gastroenterol Hepatol 27: 173-180, 2012.
40. Seo DD, Lee HC, Kim HJ, *et al*: Neural cadherin overexpression is a predictive marker for early postoperative recurrence in hepatocellular carcinoma patients. J Gastroenterol Hepatol 23: 1112-1118, 2008.
41. Hu L, Lau SH, Tzang CH, *et al*: Association of Vimentin overexpression and hepatocellular carcinoma metastasis. Oncogene 23: 298-302, 2004.
42. Pan TL, Wang PW, Huang CC, Yeh CT, Hu TH and Yu JS: Network analysis and proteomic identification of vimentin as a key regulator associated with invasion and metastasis in human hepatocellular carcinoma cells. J Proteomics 75: 4676-4692, 2012.
43. Miyoshi A, Kitajima Y, Kido S, *et al*: Snail accelerates cancer invasion by upregulating MMP expression and is associated with poor prognosis of hepatocellular carcinoma. Br J Cancer 92: 252-258, 2005.
44. Shah SA, Tan JC, McGilvray ID, *et al*: Does microvascular invasion affect outcomes after liver transplantation for HCC? A histopathological analysis of 155 consecutive explants. J Gastrointest Surg 11: 464-471, 2007.
45. Zheng SS, Xu X, Wu J, *et al*: Liver transplantation for hepatocellular carcinoma: Hangzhou experiences. Transplantation 85: 1726-1732, 2008.
46. Mergental H, Adam R, Ericzon BG, *et al*: Liver transplantation for unresectable hepatocellular carcinoma in normal livers. J Hepatol 57: 297-305, 2012.
47. Sandhu L, Sandroussi C, Guba M, *et al*: Living donor liver transplantation versus deceased donor liver transplantation for hepatocellular carcinoma: comparable survival and recurrence. Liver Transpl 18: 315-322, 2012.
48. Chan SC, Fan ST, Chok KS, *et al*: Survival advantage of primary liver transplantation for hepatocellular carcinoma within the up-to-7 criteria with microvascular invasion. Hepatol Int: Oct 21, 2011 (Epub ahead of print).
49. Chou CT, Chen RC, Lee CW, Ko CJ, Wu HK and Chen YL: Prediction of microvascular invasion of hepatocellular carcinoma by pre-operative CT imaging. Br J Radiol 85: 778-783, 2012.
50. Chandarana H, Robinson E, Hajdu CH, Drozhinin L, Babb JS and Taouli B: Microvascular invasion in hepatocellular carcinoma: is it predictable with pretransplant MRI? AJR Am J Roentgenol 196: 1083-1089, 2011.
51. Kim KA, Kim MJ, Jeon HM, *et al*: Prediction of microvascular invasion of hepatocellular carcinoma: usefulness of peritumoral hypointensity seen on gadoxetate disodium-enhanced hepatobiliary phase images. J Magn Reson Imaging 35: 629-634, 2012.
52. Adler M, De Pauw F, Vereerstraeten P, *et al*: Outcome of patients with hepatocellular carcinoma listed for liver transplantation within the Eurotransplant allocation system. Liver Transpl 14: 526-533, 2008.
53. Chen JW, Kow L, Verran DJ, *et al*: Poorer survival in patients whose explanted hepatocellular carcinoma (HCC) exceeds Milan or UCSF Criteria. An analysis of liver transplantation in HCC in Australia and New Zealand. HPB (Oxford) 11: 81-89, 2009.
54. D'Amico F, Schwartz M, Vitale A, *et al*: Predicting recurrence after liver transplantation in patients with hepatocellular carcinoma exceeding the up-to-seven criteria. Liver Transpl 15: 1278-1287, 2009.

HEPATOLOGY
Official Journal of the American Association for the Study of Liver Diseases

LIVER INJURY/REGENERATION

Adipose Tissue-Derived Stem Cells as a Regenerative Therapy for a Mouse Steatohepatitis-Induced Cirrhosis Model

Akihiro Seki,[1,2*] Yoshio Sakai,[1,3*] Takuya Komura,[2] Alessandro Nasti,[2] Keiko Yoshida,[2] Mami Higashimoto,[2] Masao Honda,[1] Soichiro Usui,[2] Masayuki Takamura,[2] Toshinari Takamura,[2] Takahiro Ochiya,[4] Kengo Furuichi,[5] Takashi Wada,[3] and Shuichi Kaneko[1,2]

Cirrhosis is a chronic liver disease that impairs hepatic function and causes advanced fibrosis. Mesenchymal stem cells have gained recent popularity as a regenerative therapy since they possess immunomodulatory functions. We found that injected adipose tissue-derived stem cells (ADSCs) reside in the liver. Injection of ADSCs also restores albumin expression in hepatic parenchymal cells and ameliorates fibrosis in a nonalcoholic steatohepatitis model of cirrhosis in mice. Gene expression analysis of the liver identifies up- and down-regulation of genes, indicating regeneration/repair and anti-inflammatory processes following ADSC injection. ADSC treatment also decreases the number of intrahepatic infiltrating CD11b$^+$ and Gr-1$^+$ cells and reduces the ratio of CD8$^+$/CD4$^+$ cells in hepatic inflammatory cells. This is consistent with down-regulation of genes in hepatic inflammatory cells related to antigen presentation and helper T-cell activation. *Conclusion*: These results suggest that ADSC therapy is beneficial in cirrhosis, as it can repair and restore the function of the impaired liver. (HEPATOLOGY 2013;58:1133-1142)

Cirrhosis is a serious, life-threatening advanced stage of chronic liver disease that leads to hepatic dysfunction.[1] Cirrhosis frequently develops into hepatocellular carcinoma,[2,3] which exacerbates the prognosis of patients with cirrhosis. The ultimate treatment for cirrhosis is a liver transplant,[4] which can be lethal.[5] The number of donor livers, however, is not sufficient to meet the needs of all transplant patients. Thus, a novel therapy for cirrhosis needs to be developed to improve cirrhotic liver prognosis.

The underlying pathogenesis of chronic liver disease is persistent inflammation. Advanced disease is marked by advanced fibrosis concomitant with distorted liver architecture characterized by regenerative nodules and impaired hepatic function. Advanced fibrosis in the cirrhotic liver is also a risk factor for the development of hepatocellular carcinoma.[6] Treatment of cirrhosis suppresses inflammation by eradicating hepatitis virus infection or reducing liver steatosis in nonalcoholic steatohepatitis (NASH). Decreasing liver inflammation and restoring hepatocyte function improves the prognosis.

Pluripotent mesenchymal stem cells (MSCs) differentiate into adipocyte, chondrocyte, and osteocyte lineages.[7] These cells can also differentiate into other lineages, including neurons[8] and hepatocytes.[9,10] MSCs can also regulate the immune response.[11] Thus, MSCs attract attention as a therapeutic target in the

Abbreviations: ADSCs, adipose-tissue-derived stem cells; AFP, alpha-fetoprotein; Ath+HF, atherogenic high-fat; IL, interleukin; MMP, matrix metalloproteinase; MSC, mesenchymal stem cells; NASH, nonalcoholic steatohepatitis; PBS, phosphate-buffered saline; 18S rRNA, 18S ribosomal RNA; α-SMA, alpha-smooth muscle actin.

From the [1]Department of Gastroenterology, Kanazawa University Hospital, Ishikawa, Japan; [2]Disease Control and Homeostasis, Kanazawa University, Ishikawa, Japan; [3]Department of Laboratory Medicine, Kanazawa University Hospital, Ishikawa, Japan; [4]National Cancer Research Institute, Tokyo, Japan; [5]Division of Blood Purification, Kanazawa University Hospital, Ishikawa, Japan.

Received September 27, 2012; accepted April 15, 2013.

Supported in part by subsidies from the Japanese Ministry of Education, Culture, Sports, Science and Technology and the Japanese Ministry of Health, Labor and Welfare.

**These authors contributed equally to this work.*

regeneration or repair of various impaired organs. Mesenchymal tissue from bone marrow, umbilical cord, and adipose tissue are relatively enriched with pluripotent stem cells.[12] Since the pathophysiological features of liver cirrhosis are a consequence of chronic hepatic inflammation, MSCs are especially suited to enhance regeneration and/or repair of damaged cirrhotic liver.

We have established a clinically relevant NASH cirrhotic murine model by feeding animals an atherogenic high-fat (Ath+HF) diet.[13] In this study we examined whether adipose-tissue-derived stem cells (ADSCs) can regenerate and/or repair the cirrhotic liver. We observed that injected ADSCs resided in the liver and expressed albumin, leading to restored albumin expression in hepatic parenchymal cells. ADSCs also ameliorated advanced fibrosis. Moreover, ADSCs suppressed the underlying persistent inflammation contributed by granulocytes, phagocytic cells, and T cells. These results suggest that treatment of patients with cirrhosis with ADSCs is a potentially novel approach for regenerating and/or repairing damaged cirrhotic liver tissue to restore hepatic function.

Materials and Methods

Culture of ADSCs. ADSCs were prepared as described.[14] Briefly, adipose tissue was obtained from the inguinal subcutaneous region of 10-week-old GFP-Tg male mice (a gift from Professor Okabe, Osaka University, Japan). The stem cell fraction was isolated from adipose tissue using type-I collagenase (Wako Pure Chemical Industries, Osaka, Japan) and cultured in Dulbecco's modified Eagle's medium: nutrient mixture F-12 supplemented with 10% heat-inactivated bovine serum albumin and 1% antibiotic-antimycotic solution. Cell culture reagents were purchased from Life Technologies (Carlsbad, CA).

NASH Murine Model. Female 8-week-old C57Bl/6J mice were purchased from Charles River Laboratories Japan (Yokohama, Japan). Mice were fed an Ath+HF diet composed of cocoa butter, cholesterol, cholate, and corticotropin-releasing factor-1 (Oriental Yeast Co., Tokyo, Japan) to induce steatohepatitis as reported previously.[13] Our Institutional Review Board approved the care and use of laboratory animals in all experiments.

ADSC Treatment of NASH Mice. ADSCs were harvested after six to eight passages in culture by treatment with trypsin/EDTA (Life Technologies) and passed through a 100-μm Cell Strainer mesh (BD Biosciences, San Jose, CA). Laparotomy was performed to inject 1×10^5 ADSCs or phosphate-buffered saline (PBS) into the splenic subcapsule. After ADSC treatment, the mice were anesthetized with pentobarbital (40 mg/kg; Kyoritsu Seiyaku, Tokyo, Japan), after which the liver was perfused with PBS and dissected. A portion of liver tissue was homogenized and incubated with type I collagenase (Wako Pure Chemical Industries), and hepatic parenchymal cells and inflammatory cells were separated with Percoll (GE Healthcare UK, Buckinghamshire, UK). $CD4^+$ T cells were isolated from hepatic inflammatory cells using a magnetic sorting system, the $CD4^+$ T cell Isolation Kit II (Miltenyi Biotec, Gladbach, Germany).

Histology and Immunohistochemical Staining. Liver tissue was preserved with formalin for paraffin embedding or embedded in OCT compound and frozen for sectioning (Sakura Finetek Japan, Tokyo, Japan). The frozen liver sections were fixed in acetone and endogenous peroxidase activity blocked with 3% hydrogen peroxide solution. After washing in PBS, the sections were incubated with a rabbit anti-CD11b antibody (BD Pharmingen, San Diego, CA) and a rabbit anti-Gr-1 antibody (eBioscience, San Diego, CA) overnight at 4°C. The slides were then washed and incubated with Histofine mouse MAXPO (Nichirei Bioscience, Tokyo, Japan) for 1 hour at room temperature. The immune complex was visualized by incubating with diaminobenzidine for 5 minutes. The paraffin-embedded sections were stained with a rabbit-anti-GFP antibody (Millipore, Billerica, MA), a rabbit anti-α-smooth muscle actin (α-SMA) antibody (Abcam, Cambridge, UK), and a rabbit anticollagen IV antibody (Abcam). Secondary antibody development was performed with diaminobenzidine as described above. In some experiments, the sliced

Address reprint requests to: Shuichi Kaneko, 13-1 Takara-machi, Kanazawa, Ishikawa 920-8641, Japan. E-mail: skaneko@m-kanazawa.jp; fax: +81-76-234-4250.

View this article online at wileyonlinelibrary.com.
DOI 10.1002/hep.26470
Potential conflict of interest: Nothing to report.
Additional Supporting Information may be found in the online version of this article.

sections were double-stained with a combination of a goat antimouse serum albumin antibody (Abcam) and a rabbit anti-GFP antibody followed by the secondary antibody and development as described above. To quantify fibrosis, paraffin-embedded sections were stained with Azan and viewed microscopically, after which the stained area was calculated using an image-analysis system (BIOREVO BZ-9000 and BZ-H1C, Keyence Japan, Osaka, Japan).

Flow Cytometry. Isolated hepatic inflammatory cells were incubated in PBS supplemented with 2% bovine serum albumin (Sigma-Aldrich, St. Louis, MO) for 10 minutes at 4°C. The cells were incubated with fluorescein isothiocyanate (FITC)-conjugated anti-CD4 (eBioscience) and phycoerythrin (PE)-conjugated anti-CD8 antibodies (eBioscience) for 30 minutes at 4°C before examination using a FACSCalibur cytometer (BD Biosciences). Similarly, ADSCs were incubated with PE-conjugated CD90 (Beckman Coulter, Fullerton, CA), or PE-conjugated CD105 (Miltenyi Biotec). The data were analyzed using the FlowJo software (Tree Star, Ashland, OR).

DNA Microarray Analysis. Isolated RNAs were amplified and labeled with Cy3 using a QuickAmp Labeling Kit (Agilent Technologies, Santa Clara, CA) in accordance with the manufacturer's protocol. cRNA (825 ng) was hybridized onto a Whole Mouse Genome 4 × 44K Array (Agilent Technologies). The hybridized microarray slide was scanned using a DNA microarray scanner (model G2505B; Agilent Technologies).

Gene expression analysis was carried out using GeneSpring analysis software (Agilent Technologies). Each measurement was divided by the 75th percentile of all measurements in that sample to normalize per chip. Hierarchical clustering and principal component analysis of gene expression was performed. Welch's t test with Benjamini and Hochberg's false-discovery rate were used to identify differentially expressed genes in the groups of interest. Analysis of biological processes was performed using the MetaCore software suite (GeneGo, San Diego, CA). BRB array tools (http://linus.nci.nih.gov/BRB-ArrayTools.html) were also used for unsupervised clustering or one-way clustering analysis. Microarray data were deposited in the NBCI Gene Expression Omnibus (GSE ID: GSE40395).

Statistical Analysis. GraphPad Prism (v. 5.0; GraphPad Software, La Jolla, CA) was used to perform a Mann-Whitney U test to compare data between two groups, and differences were considered statistically significant at $P < 0.05$.

All other materials and methods are described in the Supporting Information.

Results

Characteristics of the NASH Mouse Model. The pathological and clinical features of cirrhosis in patients are not well replicated by the majority of chemically induced murine cirrhotic liver models. We have established steatohepatitis as a cirrhotic liver mouse model by feeding mice an Ath+HF diet.[13] When mice were fed this diet for 34 weeks, hepatocytes developed steatosis, Mallory-Denk bodies, and ballooning (Fig. 1A,B), which are identical to typical pathological features of clinical NASH.[15] Albumin expression in parenchymal cells of the cirrhotic liver significantly decreased in mice fed the Ath+HF diet for 24 weeks (Fig. 1C), while alpha-fetoprotein (AFP) expression was not affected (Fig. 1D). Fibrosis developed and reached maximal levels after 34 weeks of feeding the Ath+HF diet (Fig. 1E,F). Immunohistochemical staining for immunomodulatory cells showed an increased number of Gr-1$^+$ cells in the liver of the steatohepatitis mice fed the Ath+HF diet for 12, 34, and 70 weeks (Fig. 2A,B). The number of CD11b$^+$ cells in the liver also increased and reached maximal levels after 34 weeks of feeding the Ath+HF diet (Fig. 2C,D). Thus, the murine cirrhosis model established by an Ath+HF diet mimics the features of clinical NASH.

Effect of ADSCs Treatment on Liver Albumin Expression and Fibrosis. Adipose tissue contains MSCs, which have the potential to differentiate into several types of cell lineages[10,14] and to act as immunomodulators.[11] In this study, we isolated stromal cells from inguinal adipose tissue of GFP-expressing transgenic (GFP-Tg) mice as ADSCs and expanded them in culture. The majority of these cells expressed CD90 and CD44, known surface markers of mesenchymal cells (Supporting Fig. 1A). A proportion of the expanded ADSCs also expressed CD105 (Supporting Fig. 1B), which has been recognized as a representative surface marker of MSCs.[11]

We evaluated whether ADSCs could provide a therapeutically beneficial treatment for liver cirrhosis in steatohepatitis mice. We injected 1 × 10^5 GFP-ADSCs by way of the spleen/portal vein in mice fed the Ath+HF diet for 32 weeks. We observed that the GFP-ADSCs resided in all lobes of the liver at 3, 7, and 14 days after injection (Fig. 3A,B). Importantly, immunohistochemical staining showed that GFP$^+$ cells in the cirrhotic liver expressed higher levels of albumin than did the surrounding parenchymal cells (Fig. 3C).

We also injected 1 × 10^5 or 2 × 10^4 GFP-ADSCs twice every 2 weeks by way of the splenic/portal vein

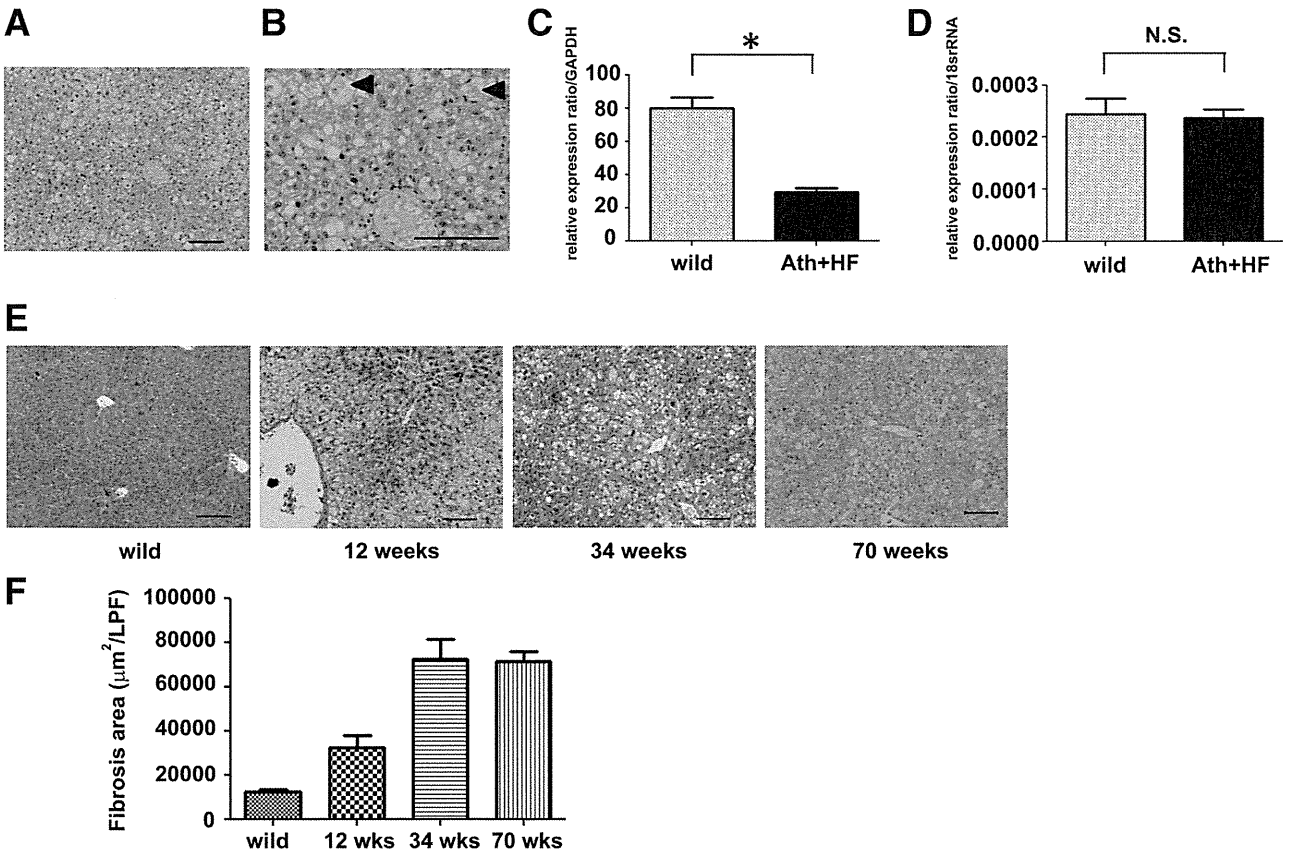

Fig. 1. Characteristics of the steatohepatitis murine model. Eight-week-old C57Bl/6 female mice were fed an Ath+HF diet. Liver tissue was obtained after 34 weeks, sectioned, and histologically examined with hematoxylin and eosin staining in (A,B) mice fed an Ath+HF diet for 34 weeks. Arrowheads indicate a Mallory-Denk body in a hepatocyte with ballooning. Parenchymal cells were isolated from 32-week-old C57Bl/6 wild-type female mice or Ath+HF mice that started the diet at 8 weeks old and continued for 24 weeks. Expression of (C) albumin and (D) AFP was assessed by reverse-transcription polymerase chain reaction (RT-PCR), n = 4, $*P < 0.05$. (E) Fibrosis was histologically examined with Azan staining in liver tissue of mice fed the Ath+HF diet for 12, 34, and 70 weeks. (F) Fibrosis areas of mice at 12, 34, and 70 weeks per ×100 low-power field were calculated for five visual fields. Bars: standard error. Scale bars = 100 μm.

in mice fed an Ath+HF diet for 32 or 36 weeks, respectively. Two weeks after the last injection the mice were euthanized and the therapeutic effects were assessed. The expression of albumin (Fig. 4A) was restored in hepatic parenchymal cells of cirrhotic mice at 2 weeks after the last injection, suggesting that ADSC treatment restored parenchymal cell function. The expression of AFP was also increased by ADSC treatment (Fig. 4B), implying enhanced regeneration of hepatic parenchymal cells. Similar effects were observed with a reduced number of (2×10^4) GFP-ADSCs (Supporting Fig. 2A,B).

We also assessed the effect of ADSC injection on fibrosis in cirrhotic mice. Liver tissue stained with Azan and anticollagen type IV antibody showed that ADSC administration reduced fibrosis compared to control animals (Fig. 5A,B; Supporting Fig. S3A,B). We also evaluated immunohistochemical staining of α-SMA, a marker of stellate cells, which are largely responsible for developing fibrosis. These results demonstrated that the number of α-SMA$^+$ cells was reduced by ADSC treatment (Fig. 5C-E), suggesting that ADSCs suppress the activity of stellate cells and ameliorate liver fibrosis.

Gene Expression Profiling of Cirrhotic Livers Following ADSC Treatment. We examined the gene expression profile of the livers in the NASH mouse model of cirrhosis by DNA microarray to determine whether administration of ADSCs was therapeutically beneficial. We identified expression of 1,249 gene probes that were significantly affected by ADSC injection. Clustering analysis of gene expression using these gene probes distinguished between ADSCs-treated mice and PBS-treated mice (Fig. 6A). Among 1,249 genes, 797 were up-regulated and 452 were down-regulated by ADSC treatment. Regarding matrix metalloproteinase (MMP), expressions of MMP-8 and MMP-9 were enhanced in the liver of NASH mice treated with PBS compared to the wild type; this enhancement was removed by ADSC treatment

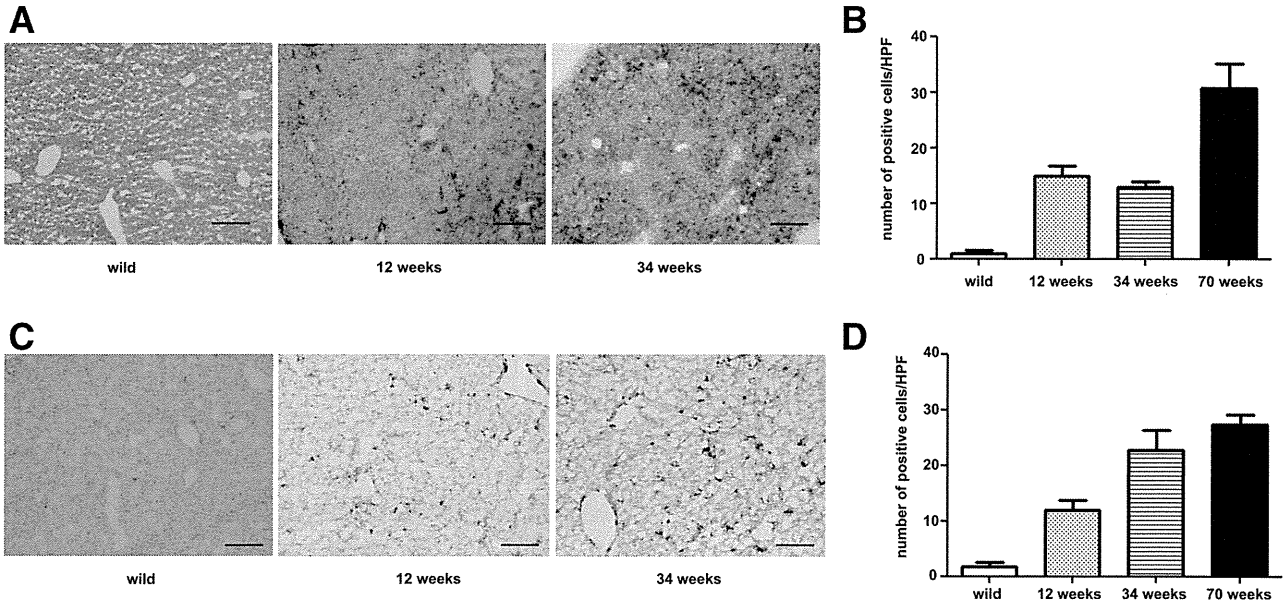

Fig. 2. Immunohistochemical staining of a steatohepatitis liver. Eight-week-old female C57Bl/6 female mice were fed an Ath+HF diet. Liver tissue was obtained from these mice or from wild-type animals after 12, 34, and 70 weeks. Immunohistochemical staining was performed for (A) Gr-1$^+$ or (C) CD11b$^+$ cells and the number of positive cells in a high-power field was counted for five visual fields for (B) Gr-1 or (D) CD11b at each timepoint.

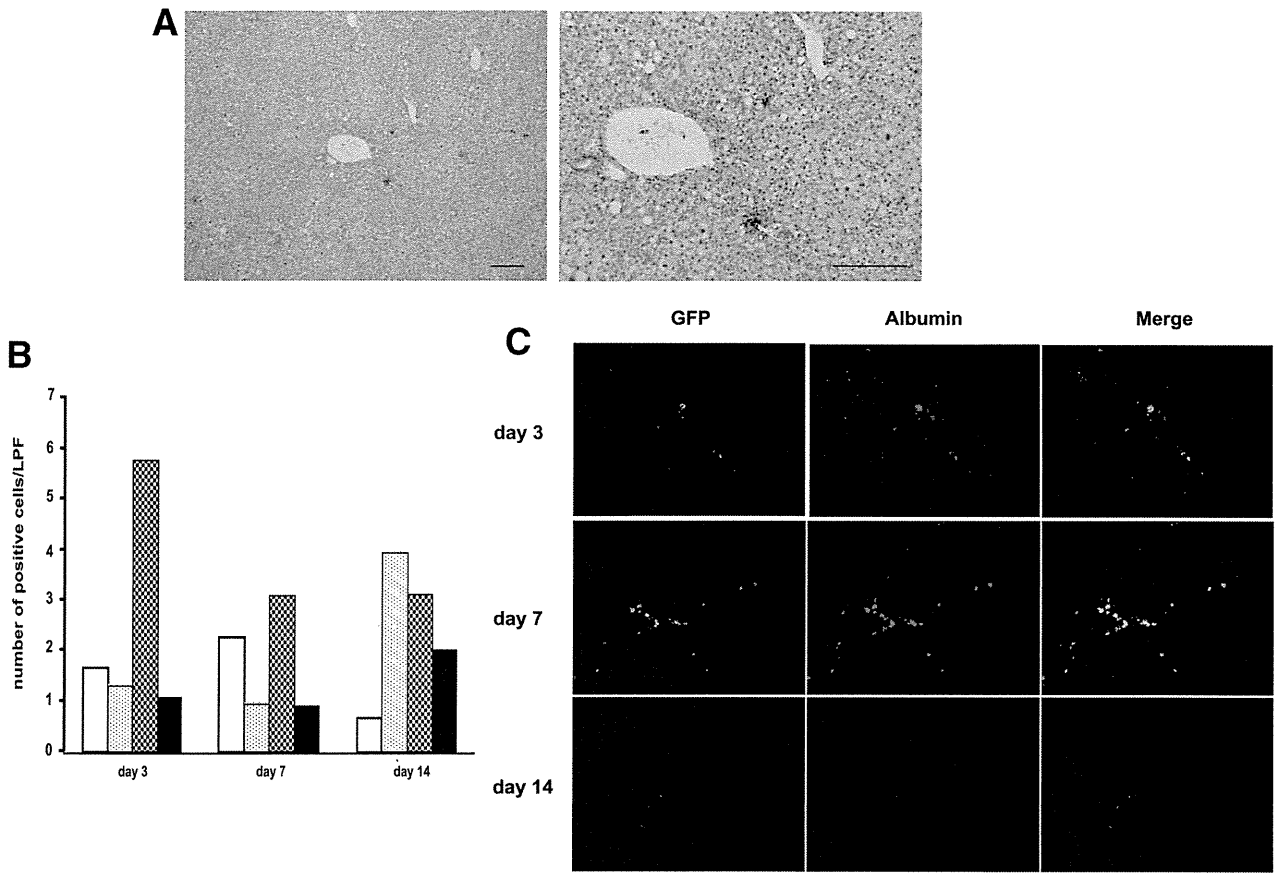

Fig. 3. Distribution of ADSCs and albumin expression in the livers of steatohepatitis mice. ADSCs from GFP-Tg mice (1×10^5) were injected into the splenic subcapsule of cirrhotic C57Bl/6 mice fed the Ath+HF diet for 32 weeks. After 3, 7, and 14 days, liver tissue was obtained and examined by immunohistochemical staining for (A) GFP; Scale bars = 100 μm. (B) GFP$^+$ cells in the liver were counted per ×100 low-power field and five visual fields were calculated. White bar, caudate lobe; dotted bar, left lobe; hatched bar, middle lobe; black bar, right lobe. (C) Immunohistochemical staining for GFP or albumin antibody. Magnification, ×100.

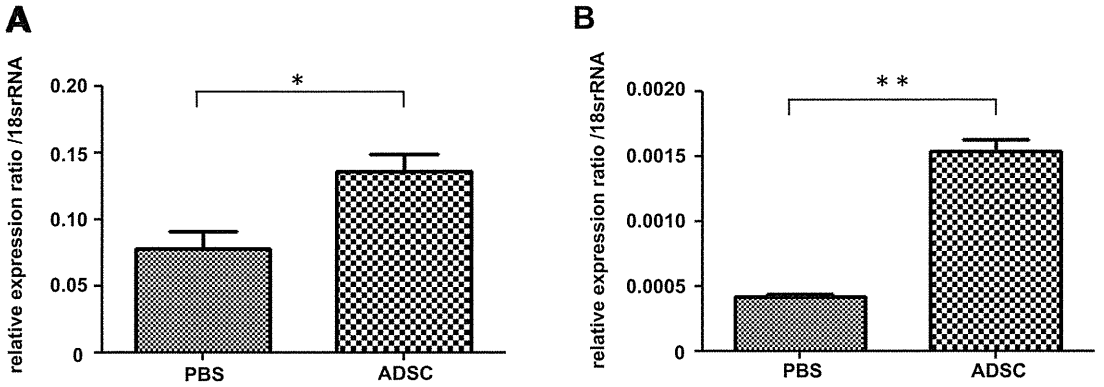

Fig. 4. Albumin and AFP expression in hepatic parenchymal cells. ADSCs from GFP-Tg mice (1×10^5) were injected twice every 2 weeks into the splenic subcapsule of cirrhotic C57Bl/6 mice fed an Ath+HF diet for 32 weeks. Control mice received PBS injections. Two weeks after the last injection, liver tissue was obtained and parenchymal cells were isolated for real-time PCR. Expressions of (A) albumin and (B) AFP were normalized relative to that of 18S ribosomal RNA (rRNA); $*P < 0.05$, $**P < 0.01$.

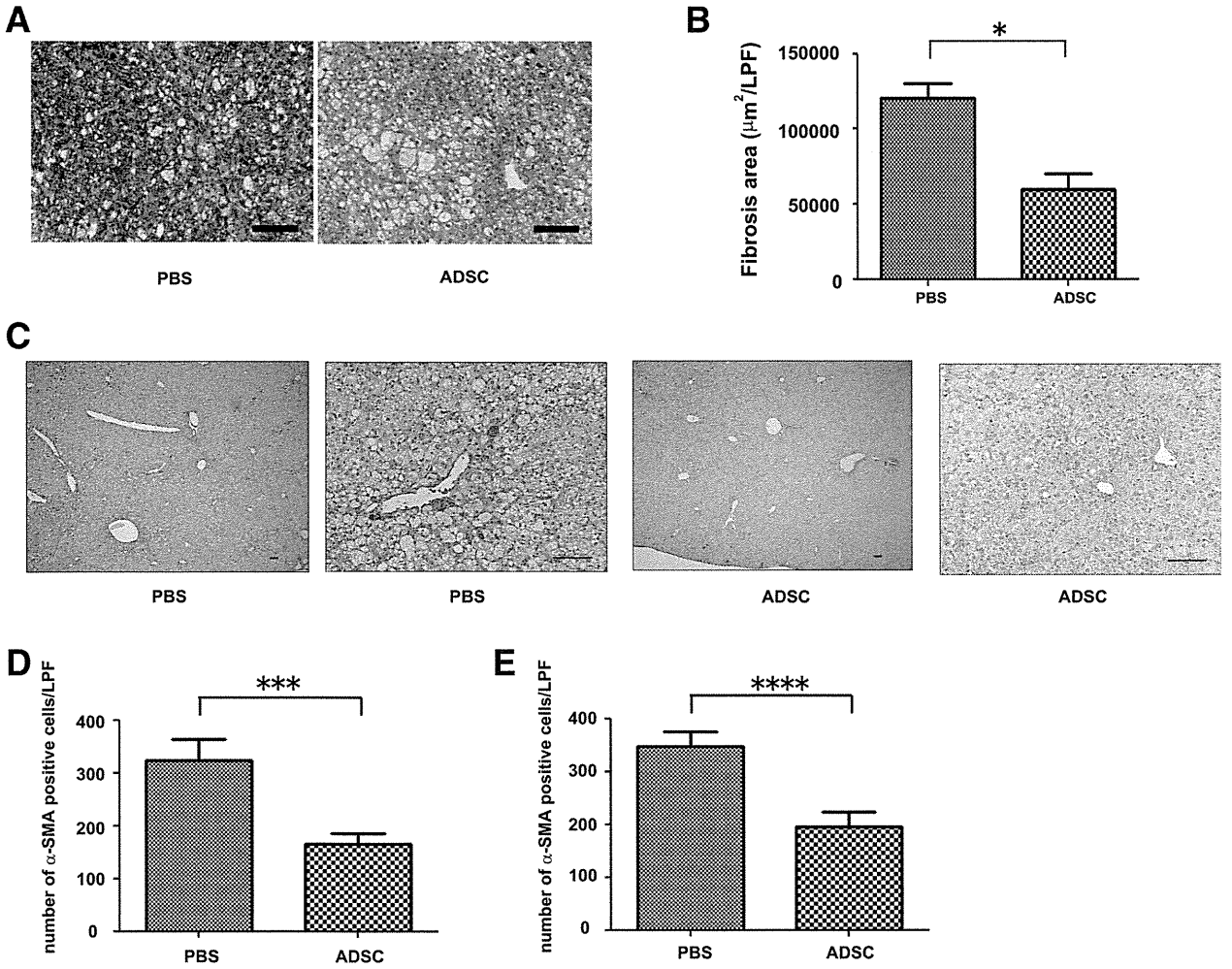

Fig. 5. Effect of ADSCs on liver fibrosis. ADSCs from GFP-Tg mice (1×10^5) were injected twice every 2 weeks into the splenic subcapsule of cirrhotic C57Bl/6 mice fed the Ath+HF diet for 32 weeks. Control mice received PBS injections. (A) Two weeks after the last injection, liver tissue was obtained, sectioned, and histologically examined with hematoxylin and eosin staining. (B) Fibrosis was examined by Azan staining and fibrotic area was quantified by image-analysis. (C) Immunohistochemical staining of liver sections for α-SMA. Scale bars = 100 μm. (D,E) The number of α-SMA+ cells in liver tissues obtained 1 (D) or 2 weeks (E) after the last ADSC injection determined by microscopy of five low-power fields (×100); $***P < 0.005$, $****P = 0.0001$.

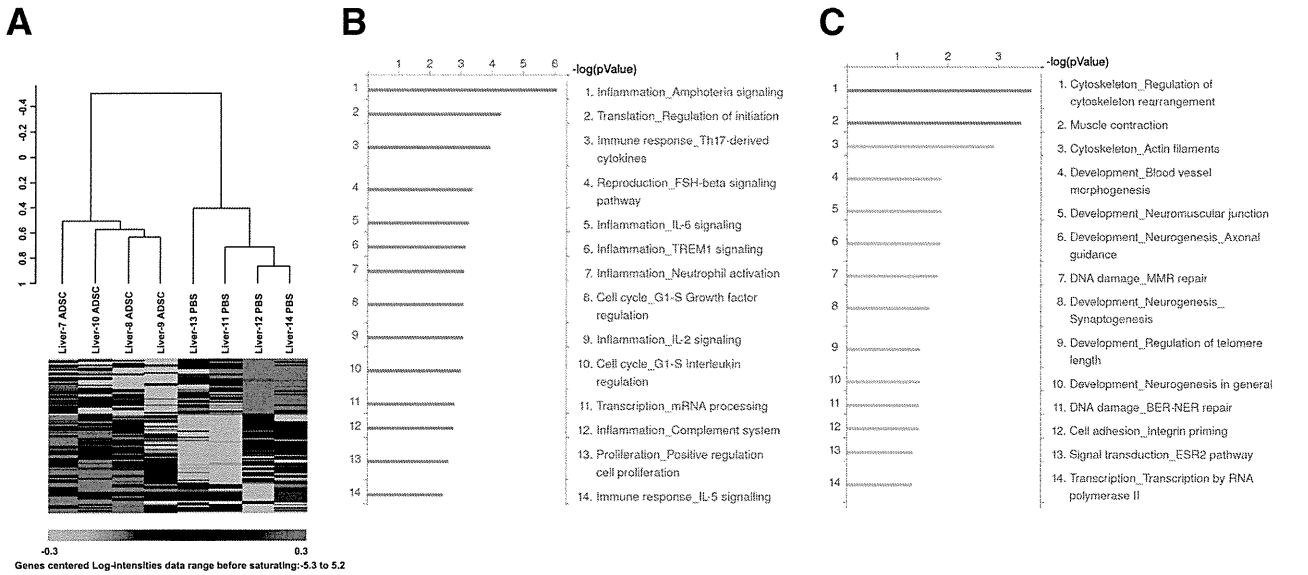

Fig. 6. Hepatic gene expression analysis. ADSCs from GFP-Tg mice (1×10^5) were injected twice every 2 weeks into the splenic subcapsule of cirrhotic C57Bl/6 mice fed an Ath+HF diet for 40 weeks. Control mice received PBS injections. Two weeks later, liver tissue was subjected to RNA isolation and gene expression using DNA microarrays. (A) Unsupervised clustering analysis was performed using probes for 1,249 genes whose expression differed significantly between the PBS and ADSC groups. (B) The biological processes of 452 genes whose expression was down-regulated in the ADSCs group compared to the PBS group were analyzed. (C) The biological processes of 797 genes whose expression was up-regulated in the ADSCs group compared to the PBS group were analyzed.

(Supporting Fig. S4). Biological process analysis indicated that the down-regulated genes were primarily related to inflammation and the immune response (Fig. 6B), and the up-regulated genes were related to tissue construction and development (Fig. 6C). Thus, gene expression analysis of liver tissue demonstrated that ADSCs treatment caused anti-inflammatory effects, as well as regeneration/repair effects, in the livers of a NASH mouse model of cirrhosis.

Anti-inflammatory Effects of ADSC Treatment. The fundamental underlying pathophysiology of steatohepatitis-induced cirrhosis is persistent hepatic inflammation caused by steatosis in hepatocytes.[16] We examined how ADSCs affected persistent inflammation of the liver in NASH mice at 2 weeks after the last injection of ADSCs. Immunohistochemical staining showed that the number of $CD11b^+$ cells accumulating in the livers of cirrhotic mice decreased with ADSC treatment compared to those of PBS-treated mice (Fig. 7A). The number of $Gr\text{-}1^+$ cells in cirrhotic liver also decreased with ADSC treatment (Fig. 7A), suggesting that ADSCs affect granulocytes and antigen-presenting cell lineage.

We further examined whether ADSC treatment affected the lymphocyte lineage of T cells, since they also play an important role in immune regulation of steatohepatitis.[17] We isolated lymphocytes from the livers of mice treated with ADSCs and examined the $CD4^+$ and $CD8^+$ T cells using flow cytometry. $CD8^+$ T cells were found predominantly in cirrhotic mice treated with PBS (Fig. 7B,C). However, when the mice were treated with ADSCs the number of $CD4^+$ T cells increased and was comparable to that of $CD8^+$ T cells, indicating that ADSC treatment affected T-cell subpopulations.

Gene Expression Profiling of Hepatic Inflammatory Cells Following ADSC Treatment. We further examined how injected ADSCs affected hepatic inflammatory cell gene expression by using DNA microarrays. By filtering the results from 5,065 gene probes, completely discernible clusters of gene expression were formed between ADSC- and PBS-treated animals (Fig. 8A). We identified the expression of 873 genes that were significantly up-regulated at least 2-fold with ADSC injection and 658 genes that were down-regulated. Most of the chemokines and cytokines whose expression was significantly affected by ADSCs were down-regulated (Supporting Table S1). Using the publicly available gene expression database for hematopoietic cells (GSE27787) and various types of helper T cells (GSE14308), we examined features of these affected genes in the context of immunomodulatory cells. Among the hematopoietic cells, genes with available symbol annotation were predominately $Gr\text{-}1^+$ and $CD11b^+$ cells from granulocyte and macrophage lineages (Fig. 8B). Among helper T-cell populations,

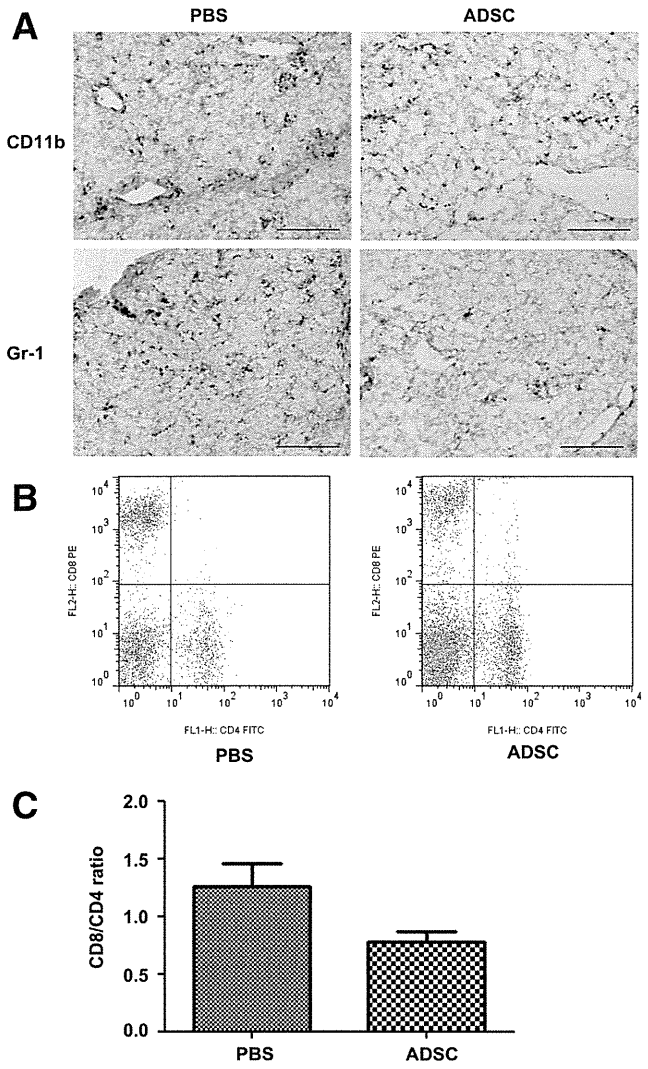

Fig. 7. Effect of ADSCs on inflammatory cells in the cirrhotic liver. ADSCs from GFP-Tg mice (1×10^5) were injected twice every 2 weeks into the splenic subcapsule of cirrhotic C57Bl/6 mice fed the Ath+HF diet for 32 weeks. Control mice received PBS injections. Two weeks later, liver tissue was obtained and immunohistochemical staining of (A) $CD11b^+$ and (B) $Gr\text{-}1^+$ cells was performed. Inflammatory cells in the liver were also isolated and stained with FITC-labeled anti-CD4 and PE-labeled CD8 antibodies. (C) The ratio of $CD8^+$ cells to $CD4^+$ cells was calculated. N = 4 ± standard error.

annotated genes included activated Th1, Th2, and Th17 cell types (Fig. 8C). We also isolated $CD4^+$T cells from hepatic inflammatory cells obtained from NASH mice fed an Ath+HF diet for 12 weeks, then treated with ADSC. Expressions of the Th1, Th2, and Th17 cytokines, interferon-γ, interleukin (IL)−4, IL-10, and IL-17, the Th17-related cytokine transforming growth factor beta (TGF-β), and Foxp3, a representative transcription factor of regulatory T cells, were down-regulated by ADSC treatment (Supporting Fig. S5).

These results suggest that ADSC treatment suppresses inflammation in the NASH mouse model primarily by down-regulating granulocytes, antigen-presenting cells, and activated helper T cells.

Discussion

This study investigated the therapeutic effect of ADSCs in a NASH murine model of cirrhosis. This model is relevant to clinical NASH, with similar pathological features established by an atherogenic high-fat diet, including the appearance of steatosis, ballooning, and Mallory-Denk bodies in hepatocytes, infiltration of inflammatory cells, and pericellular fibrosis. Our results demonstrate that ADSC injection is therapeutically beneficial for cirrhosis in this murine model through restoration of albumin expression in hepatic parenchymal cells, amelioration of fibrosis, and suppression of persistent hepatic inflammation.

Gene expression analysis of the liver in this cirrhotic mouse model revealed that ADSC injection affects biological processes relating to anti-inflammatory and regeneration/repair pathways. The anti-inflammatory effects are mediated by ADSC targeting of $Gr\text{-}1^+$, $CD11b^+$, and helper T-cell lineages. In patients with clinical NASH, the ratio of neutrophils to lymphocytes increases,[18] suggesting that granulocytes are involved in the pathogenesis of NASH. The NASH murine model used in this study produced an increased $CD8^+/CD4^+$ T-cell ratio, which is also comparable to clinical NASH patient pathology.[19] Gene expression analysis of liver tissue and hepatic inflammatory cells from NASH mice showed that Th1-, Th2-, and Th17-related genes were down-regulated by ADSC treatment. Helper T-cell activation skewed to produce Th1 cytokines is pathogenic in steatohepatitis.[20,21] In particular, Th17 is emerging as an important source of IL-17 family cytokines[22] and is involved in the hepatic inflammation in NASH.[23] Helper T cells producing Th2 cytokines such as IL-4, 5, and 13 contribute to fibrosis.[24] We conclude that activated T helper cells are responsible for the pathogenesis of steatohepatitis in the NASH murine model used in this study and that ADSCs suppress pathogenic helper T-cell activation. However, the suppression of miscellaneous effector and regulatory helper T cells by ADSCs should be further evaluated with regard to prevention of hepatocellular carcinoma, a frequent sequela to cirrhosis, since Th1 promotes antitumor immunity and Th2 down-regulates antitumor immunity.

We also observed that ADSC treatment ameliorated fibrosis and decreased the number of α-SMA^+ stellate

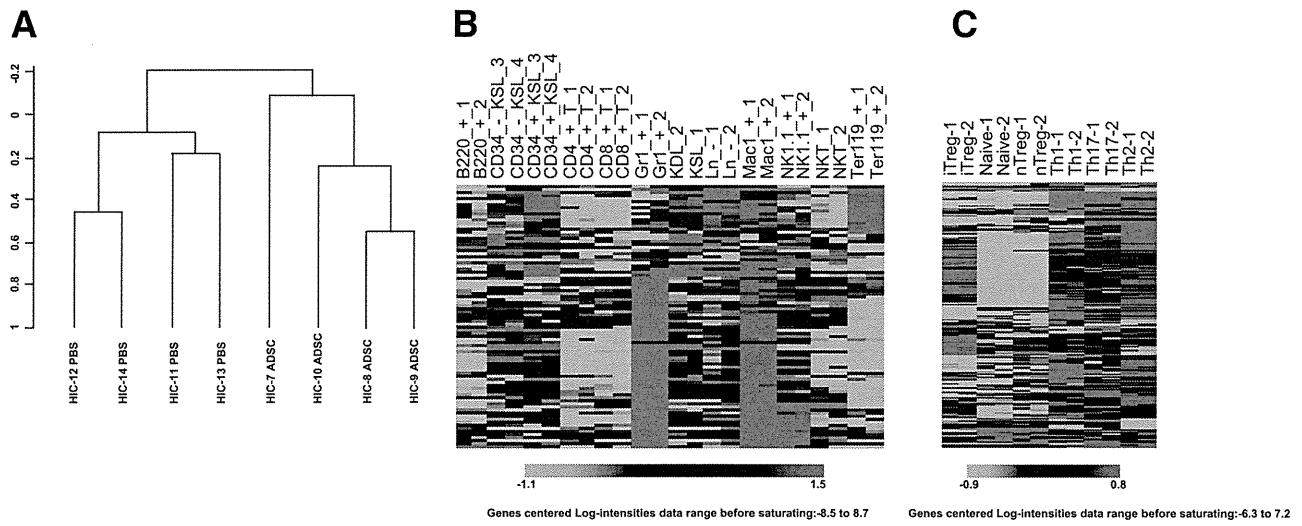

Fig. 8. Gene-expression analysis of intrahepatic inflammatory cells. ADSCs from GFP-Tg mice (1×10^5) were injected twice every 2 weeks into the splenic subcapsule of cirrhotic C57Bl/6 mice fed an Ath+HF diet for 40 weeks. Control mice received PBS injections. Inflammatory cells were isolated from the liver and gene expression examination was performed using DNA microarrays. (A) Unsupervised clustering analysis using the filtered 5,065 gene probes. HIC; hepatic inflammatory cells. (B) One-way clustering analysis using a publicly available database of hematopoietic cells (GSE27787) of 658 genes whose expression was down-regulated by ADSC treatment with available gene symbol annotations. (C) One-way clustering analysis using publicly available database of different helper T subsets (GSE14308) of 658 genes whose expression was down-regulated by ADSCs treatment with available gene symbol annotations.

cells in cirrhotic liver. When inflammation persists in the liver, fibrosis progresses due to these activated stellate cells, which are almost identical to myofibroblasts and produce extracellular matrix. Stellate cells are activated by miscellaneous factors including TGF-β and platelet-derived growth factor,[25] produced mostly from Kupffer cells. Helper T cells expressing Th2 cytokines are also involved in the development of fibrosis. Gene expression analysis of the cirrhotic livers indicated that ADSC treatment suppressed Th2-type helper T cells. Although details of how these molecules mediate fibrosis development have yet to be examined in the current NASH murine model, the antifibrotic effect of ADSCs is achieved in part by suppressing Th2-type helper T cells. We found that MMP-8 and MMP-9 enhancement in the NASH-cirrhotic liver was ameliorated by ADSC treatment. MMP-9 expression is related to the inflammation typical of steatohepatitis[26] and can ameliorate the hepatic fibrosis induced by carbon tetrachloride.[27] Further studies are needed to clarify the role of MMPs in the pathogenesis of cirrhosis as well as to explore novel therapies for this condition.

Pluripotent MSCs differentiate into several cell lineages and are a promising avenue for regenerative therapy of various impaired organs, including the liver. Although ADSCs were observed in cirrhotic livers at up to 2 weeks after injection and expressed albumin, the numbers of resident cells were not sufficient to supplement hepatic function. Therefore, pluripotency, as well as the anti-inflammatory and antifibrotic effects of ADSCs, are important for their regenerative/repair effects in liver cirrhosis. Rather than studying the effects of ADSCs on early-stage steatohepatitis, we treated mice with endstage cirrhosis with ADSCs to observe their therapeutic effects. Our results demonstrated that ADSCs can effectively resolve chronic fibrosis and decrease inflammation, thereby restoring hepatic function in endstage cirrhotic mice, implying the usefulness of this therapy as an alternative to liver transplantation.

In conclusion, ADSCs proved therapeutically beneficial and clinically relevant in regenerative therapy of a murine steatohepatitis-cirrhosis model. Clinical application of ADSCs in the treatment of cirrhosis is expected to provide a novel alternative regenerative/repair therapy for patients with cirrhosis.

References

1. D'Amico G, Garcia-Tsao G, Pagliaro L. Natural history and prognostic indicators of survival in cirrhosis: a systematic review of 118 studies. J Hepatol 2006;44:217-231.
2. Llovet JM, Burroughs A, Bruix J. Hepatocellular carcinoma. Lancet 2003;362:1907-1917.
3. Fattovich G, Stroffolini T, Zagni I, Donato F. Hepatocellular carcinoma in cirrhosis: incidence and risk factors. Gastroenterology 2004;127:S35-50.
4. Kamath PS, Kim WR. The model for end-stage liver disease (MELD). Hepatology 2007;45:797-805.
5. Stravitz RT, Carl DE, Biskobing DM. Medical management of the liver transplant recipient. Clin Liver Dis 2011;15:821-843.

6. Forner A, Llovet JM, Bruix J. Hepatocellular carcinoma. Lancet 2012;379:1245-1255.
7. Chamberlain G, Fox J, Ashton B, Middleton J. Concise review: mesenchymal stem cells: their phenotype, differentiation capacity, immunological features, and potential for homing. Stem Cells 2007;25:2739-2749.
8. Franco Lambert AP, Fraga Zandonai A, Bonatto D, Cantarelli Machado D, Pegas Henriques JA. Differentiation of human adipose-derived adult stem cells into neuronal tissue: does it work? Differentiation 2009;77:221-228.
9. Banas A, Teratani T, Yamamoto Y, Tokuhara M, Takeshita F, Osaki M, et al. Rapid hepatic fate specification of adipose-derived stem cells and their therapeutic potential for liver failure. J Gastroenterol Hepatol 2009;24:70-77.
10. Banas A, Teratani T, Yamamoto Y, Tokuhara M, Takeshita F, Quinn G, et al. Adipose tissue-derived mesenchymal stem cells as a source of human hepatocytes. HEPATOLOGY 2007;46:219-228.
11. Uccelli A, Moretta L, Pistoia V. Immunoregulatory function of mesenchymal stem cells. Eur J Immunol 2006;36:2566-2573.
12. Zuk PA, Zhu M, Ashjian P, De Ugarte DA, Huang JI, Mizuno H, et al. Human adipose tissue is a source of multipotent stem cells. Mol Biol Cell 2002;13:4279-4295.
13. Matsuzawa N, Takamura T, Kurita S, Misu H, Ota T, Ando H, et al. Lipid-induced oxidative stress causes steatohepatitis in mice fed an atherogenic diet. HEPATOLOGY 2007;46:1392-1403.
14. Furuichi K, Shintani H, Sakai Y, Ochiya T, Matsushima K, Kaneko S, et al. Effects of adipose-derived mesenchymal cells on ischemia-reperfusion injury in kidney. Clin Exp Nephrol 2012;16:579-589.
15. Brunt EM. Nonalcoholic steatohepatitis: definition and pathology. Semin Liver Dis 2001;21:3-16.
16. Cohen JC, Horton JD, Hobbs HH. Human fatty liver disease: old questions and new insights. Science 2011;332:1519-1523.
17. Inzaugarat ME, Ferreyra Solari NE, Billordo LA, Abecasis R, Gadano AC, Chernavsky AC. Altered phenotype and functionality of circulating immune cells characterize adult patients with nonalcoholic steatohepatitis. J Clin Immunol 2011;31:1120-1130.
18. Alkhouri N, Morris-Stiff G, Campbell C, Lopez R, Tamimi TA, Yerian L, et al. Neutrophil to lymphocyte ratio: a new marker for predicting steatohepatitis and fibrosis in patients with nonalcoholic fatty liver disease. Liver Int 2012;32:297-302.
19. Susca M, Grassi A, Zauli D, Volta U, Lenzi M, Marchesini G, et al. Liver inflammatory cells, apoptosis, regeneration and stellate cell activation in non-alcoholic steatohepatitis. Dig Liver Dis 2001;33:768-777.
20. Olleros ML, Martin ML, Vesin D, Fotio AL, Santiago-Raber ML, Rubbia-Brandt L, et al. Fat diet and alcohol-induced steatohepatitis after LPS challenge in mice: role of bioactive TNF and Th1 type cytokines. Cytokine 2008;44:118-125.
21. Ferreyra Solari NE, Inzaugarat ME, Baz P, De Matteo E, Lezama C, Galoppo M, et al. The role of innate cells is coupled to a Th1-polarized immune response in pediatric nonalcoholic steatohepatitis. J Clin Immunol 2012;32:611-621.
22. Ouyang W, Kolls JK, Zheng Y. The biological functions of T helper 17 cell effector cytokines in inflammation. Immunity 2008;28:454-467.
23. Tang Y, Bian Z, Zhao L, Liu Y, Liang S, Wang Q, et al. Interleukin-17 exacerbates hepatic steatosis and inflammation in non-alcoholic fatty liver disease. Clin Exp Immunol 2011;166:281-290.
24. Wynn TA. Fibrotic disease and the T(H)1/T(H)2 paradigm. Nat Rev Immunol 2004;4:583-594.
25. Wu J, Zern MA. Hepatic stellate cells: a target for the treatment of liver fibrosis. J Gastroenterol 2000;35:665-672.
26. Wanninger J, Walter R, Bauer S, Eisinger K, Schaffler A, Dorn C, et al. MMP-9 activity is increased by adiponectin in primary human hepatocytes but even negatively correlates with serum adiponectin in a rodent model of non-alcoholic steatohepatitis. Exp Mol Pathol 2011;91:603-607.
27. Higashiyama R, Inagaki Y, Hong YY, Kushida M, Nakao S, Niioka M, et al. Bone marrow-derived cells express matrix metalloproteinases and contribute to regression of liver fibrosis in mice. HEPATOLOGY 2007;45:213-222.

Cancer Immunol Immunother (2013) 62:1421–1430
DOI 10.1007/s00262-013-1447-1

ORIGINAL ARTICLE

Increase in $CD14^+HLA\text{-}DR^{-/low}$ myeloid-derived suppressor cells in hepatocellular carcinoma patients and its impact on prognosis

Fumitaka Arihara · Eishiro Mizukoshi · Masaaki Kitahara · Yoshiko Takata · Kuniaki Arai · Tatsuya Yamashita · Yasunari Nakamoto · Shuichi Kaneko

Received: 15 February 2013 / Accepted: 29 May 2013 / Published online: 14 June 2013

Abstract Myeloid-derived suppressor cells (MDSCs) are known as key immune regulators in various human malignancies, and it is reported that $CD14^+HLA\text{-}DR^{-/low}$ MDSCs are increased in hepatocellular carcinoma (HCC) patients. However, the host factors that regulate the frequency and the effect on the prognosis of HCC patients are still unclear. We investigated these issues and clarified the relationships between a feature of MDSCs and host factors in HCC patients. We examined the frequency of MDSCs in 123 HCC patients, 30 chronic liver disease patients without HCC, and 13 healthy controls by flow cytometric analysis. The relationships between the clinical features and the frequency of MDSCs were analyzed. In 33 patients who received curative radiofrequency ablation (RFA) therapy, we examined the impact of MDSCs on HCC recurrence. The frequency of MDSCs in HCC patients was significantly increased. It was correlated with tumor progression, but not with the degree of liver fibrosis and inflammation. In terms of serum cytokines, the concentrations of IL-10, IL-13, and vascular endothelial growth factor were significantly correlated with the frequency of MDSCs. In HCC patients who received curative RFA therapy, the frequency of MDSCs after treatment showed various changes and was inversely correlated with recurrence-free survival time. The frequency of MDSCs is correlated with tumor progression, and this frequency after RFA is inversely correlated with the prognosis of HCC patients. Patients with a high frequency of MDSCs after RFA should be closely followed and the inhibition of MDSCs may improve the prognosis of patients.

Keywords Myeloid-derived suppressor cells · Hepatocellular carcinoma · Radiofrequency ablation · Recurrence · Cancer

Abbreviations

MDSCs	Myeloid-derived suppressor cells
HCC	Hepatocellular carcinoma
CLD	Chronic liver disease
RFA	Radiofrequency ablation
TACE	Transcatheter arterial chemoembolization
PBMC	Peripheral blood mononuclear cell
Tregs	Regulatory T cells
HLA	Human leukocyte antigen
FGF	Fibroblast growth factor
CCL	Chemokine C–C motif ligand
G-CSF	Granulocyte colony stimulating factor
GM-CSF	Granulocyte macrophage colony stimulating factor
IP	Interferon gamma-induced protein
MCP	Monocyte chemoattractant protein
MIP	Macrophage inflammatory protein
PDGF	Platelet-derived growth factor
RANTES	Regulated upon activation, normal T cell expressed and secreted
TNF	Tumor necrosis factor
VEGF	Vascular endothelial growth factor

Electronic supplementary material The online version of this article (doi:10.1007/s00262-013-1447-1) contains supplementary material, which is available to authorized users.

F. Arihara (✉) · E. Mizukoshi · M. Kitahara · Y. Takata · K. Arai · T. Yamashita · S. Kaneko
Department of Gastroenterology, Graduate School of Medicine, Kanazawa University, 13-1, Takara-machi, Kanazawa, Ishikawa 920-8641, Japan
e-mail: bnkyo78@gmail.com; arihara@m-kanazawa.jp

Y. Nakamoto
Second Department of Internal Medicine, Faculty of Medical Sciences, University of Fukui, Matsuoka, Fukui, Japan

JAK Janus kinase
STAT Signal transducer and activator of transcription

Introduction

Hepatocellular carcinoma (HCC) is one of the most common malignancies and the third leading cause of cancer mortality globally [1, 2]. Current treatment options including surgical resection, radiofrequency ablation (RFA), liver transplantation, chemotherapy, transcatheter arterial chemoembolization (TACE), and sorafenib are reported to improve survival in HCC patients [3–7]. However, despite curative treatments for HCC, tumor recurrence rates remain high and the survival of those who have advanced HCC remains unsatisfactory [3–7]. Therefore, the development of new anti-tumor treatments for HCC remains an urgent and important field of research.

To overcome the limitations of these treatments, several immunotherapies have been developed as attractive strategies for HCC. In several studies of HCC immunotherapy, effective induction of immune-mediated cells by tumor antigen-derived peptides or antigen-presenting cells showed anti-tumor effects, but the population of patients who exhibited such effects was very small [8–12].

In previous studies, it was reported that many kinds of tumor generate a number of immune-suppressive mechanisms [13–15]. Recently, myeloid-derived suppressor cells (MDSCs) have been characterized as key immune regulators in various human cancers [15–24]. They show the capacity to inhibit T cell function and promote tumor development [15, 25]. Human MDSCs are a heterogeneous population that shows $CD11b^+$, $CD33^+$, HLA-$DR^{-/low}$ and can be divided into granulocytic $CD14^-$ and monocytic $CD14^+$ subtypes [26–28]. In most recent studies, it has been reported that $CD14^+$HLA-$DR^{-/low}$ MDSCs were increased in HCC patients and the cells inhibited the function of T cells through the induction of regulatory T cells (Tregs) [24]. Tregs represent 5–10 % of $CD4^+$ T cells and can suppress the activation and proliferation of $CD4^+$ and $CD8^+$ T cells [14, 29]. It was reported that an increased frequency of circulating Tregs was associated with poor survival of HCC patients [30]. Understanding the inhibitory mechanism of MDSCs and controlling their function are very important to develop more effective immunotherapy for HCC.

In this study, we investigate the host factors that are associated with the frequency of MDSCs in HCC patients and the effect of MDSCs on the prognosis of patients and clarify the relationships between a feature of MDSCs and host factors in HCC patients.

Materials and methods

Patients and healthy controls

Blood samples were obtained from a total of 123 HCC patients, 26 chronic liver disease (CLD) patients without HCC, and 13 healthy controls. The diagnosis of HCC was histologically confirmed in 68 patients. For the remaining 55 patients, diagnosis was made by dynamic CT or MRI. Patient characteristics and disease classification are shown in Suppl. table 1. All CLD patients without HCC underwent percutaneous liver biopsy to evaluate the disease severity according to the Metavir scoring system. In 33 patients treated with curative percutaneous RFA, blood samples were obtained on the day of treatment and 2–4 weeks after treatment, and we observed recurrence of these patients with periodic imaging studies. All subjects provided written informed consent to participate in this study in accordance with the Declaration of Helsinki. This study was approved by the regional ethics committee (Medical Ethics Committee of Kanazawa University).

Cell isolation and flow cytometric analysis

Peripheral blood mononuclear cells (PBMCs) were separated as described below; heparinized venous blood was diluted in phosphate-buffered saline (PBS) and loaded on Ficoll-Histopaque (Sigma, St. Louis, Mo.) in 50 ml tubes. After centrifugation at 2,000 rpm for 20 min at room temperature, PBMCs were harvested from the interphase, resuspended in PBS, centrifuged at 1,400 rpm for 10 min, and finally resuspended in complete culture medium consisting of RPMI (GibcoBRL, Grand Island, NY), 10 % heat inactivated FCS (Gibco BRL), 100 U/ml penicillin, and 100 μg/ml streptomycin (Gibco BRL). PBMCs were resuspended in RPMI 1,640 medium containing 80 % FCS and 10 % dimethyl sulfoxide and cryopreserved until use. The viability of cryopreserved PBMCs was 60–70 %. In some patients, fresh and cryopreserved PBMCs were obtained from the same sample. To determine the frequency and phenotype of MDSCs and Tregs, multicolor fluorescence-activated cell sorting analysis was carried out using the Becton–Dickinson FACSAria II system. The following anti-human monoclonal antibodies were used: anti-CD4 (Becton–Dickinson), anti-CD11b (Becton–Dickinson), anti-CD14 (Becton–Dickinson), anti-CD15 (Becton–Dickinson), anti-CD25 (Becton–Dickinson), anti-CD33 (Becton–Dickinson), anti-CD127 (Becton–Dickinson), and anti-HLA-DR (Becton–Dickinson).

Suppression assay

$CD14^+$HLA-$DR^{-/low}$ MDSCs and $CD14^+$HLA-DR^+ cells were sorted using the Becton–Dickinson FACSAria II

system. 2×10^4 PBMCs were cultured and stimulated with 1 μg/ml plate-bound anti-CD3 (eBioscience) and 1 μg/mL soluble anti-CD28 (eBioscience) in 96-well round-bottomed plates. 24 h later, to determine the suppressive ability of MDSCs, increasing concentrations of MDSCs were added to the stimulated PBMCs. Proliferation was measured by ^{3}Hincorporation after 72 h. [^{3}H] thymidine was added, and cell proliferation was measured by incorporation of radiolabeled thymidine for 24 h.

Cytokine and chemokine profiling

Blood samples were collected from patients at the same time of PBMC isolation. After centrifugation at 3,000 rpm for 10 min at 4 °C, serum fractions were obtained and stored at −20 °C until use. Serum levels of various cytokines and chemokines were measured using the Bio-Plex Protein Array System. Briefly, frozen serum samples were thawed at room temperature and diluted 1:4 in sample diluents; 50 μl aliquots of the diluted sample was added in duplicate to the wells of 96-well microtiter plates containing the coated beads for a validated panel of human cytokines and chemokines according to the manufacturer's instructions. The following 27 cytokines and chemokines were targeted: IL-1β, IL-1 receptor antagonist (IL-1Ra), IL-2, IL-4, IL-5, IL-6, IL-7, IL-8, IL-9, IL-10, IL-12(p70), IL-13, IL-15, IL-17, basic fibroblast growth factor (FGF), eotaxin (chemokine C–C motif ligand (CCL) 11), G-CSF, GM-CSF, IFN-γ, interferon gamma-induced protein (IP)-10, monocyte chemoattractant protein (MCP)-1, macrophage inflammatory protein (MIP)-1α, MIP-1β, platelet-derived growth factor (PDGF)-BB, regulated upon activation, normal T cell expressed and secreted (RANTES), TNF-α, and vascular endothelial growth factor (VEGF). Nine standards (ranging from 0.5 to 32,000 pg/ml) were used to generate calibration curves for each cytokine. Data acquisition and analysis were performed using Bio-Plex Manager software version 4.1.1.

Statistical analysis

Data are expressed as the mean ± SD. Chi-squared test with Yates' correction, unpaired t test, Mann–Whitney U test, and Kruskal–Wallis were used for univariate analysis of two groups that were classified according to the frequency of MDSCs. The probability of tumor recurrence-free survival was estimated using the Kaplan–Meier method. The Mantel-Cox log-rank test was used to compare curves between groups. The prognostic factors for tumor recurrence-free survival were analyzed for statistical significance by the Kaplan–Meier method (univariate) and the Cox proportional hazard model (multivariate). Variables with $p < 0.1$ were entered into multivariate logistic regression analysis. A level of $p < 0.05$ was considered significant.

Results

$CD14^+HLA\text{-}DR^{-/low}$ MDSCs are increased in the peripheral blood of HCC patients

We analyzed the peripheral blood of 123 patients with HCC, 26 CLD patients without HCC, and 13 healthy donors for the prevalence of $CD14^+HLA\text{-}DR^{-/low}$ MDSCs. Because the PBMCs are tested after Ficoll, some cells may be lost. Therefore, we examined the population of MDSCs as a percentage of total $CD14^+$ cells by flow cytometry after cell surface labeling for the expression of HLA-DR (Fig. 1a). $CD14^+HLA\text{-}DR^{-/low}$ population in PBMCs of HCC patients represented 3.2–56.8 % of the $CD14^+$ cells. The frequency of $CD14^+HLA\text{-}DR^{-/low}$ MDSCs/$CD14^+$ cells in cryopreserved PBMCs correlated with that in fresh PBMCs (Fig. 1b). Therefore, we analyzed the frequency of $CD14^+HLA\text{-}DR^{-/low}$ MDSCs/$CD14^+$ cells using cryopreserved PBMCs.

To confirm the function of these cells, sorted $CD14^+HLA\text{-}DR^{-/low}$ MDSCs and $CD14^+HLA\text{-}DR^+$ (control) cells were added at different ratios to autologous anti-CD3/CD28-stimulated PBMCs, and the proliferation was measured by ^{3}Hincorporation. $CD14^+HLA\text{-}DR^{-/low}$ MDSCs of HCC patients significantly decreased autologous PBMC proliferation (Fig. 1c). On the other hand, $CD14^+HLA\text{-}DR^+$ (control) cells could not suppress the autologous PBMC proliferation.

As shown in Fig. 1d, the frequency of MDSCs was significantly higher in HCC patients (19.0 %) than in healthy donors (9.4 %) ($p < 0.01$). Overall frequencies of $CD14^+$ cells did not differ significantly between the groups (Fig. 1e). Individual frequencies of MDSCs of all the patients and healthy donors are represented as scatter plots (Fig. 2a). The frequency of MDSCs was correlated with the stage of HCC (stage III and IV: 22.3 % ($n = 46$) vs. stage I and II: 17.0 % ($n = 77$), $p < 0.01$) and was significantly higher in HCC patients than CLD patients without HCC and healthy donors. Interestingly, there was no difference between CLD patients without HCC and healthy donors. Moreover, these numbers did not change depending on the degree of fibrosis or inflammatory activity of the liver (Fig. 2b, c).

In previous reports, granulocytic MDSCs were defined in combination with several surface markers including CD14, CD15, CD11b, CD33, CD66b, and HLA-DR in several cancers. Therefore, we examined the frequency of $CD15^+CD14^-CD11b^+CD33^+$ cells in 37 HCC patients and 11 healthy donors (Suppl. figure 1A). Although there was no statistical significant difference, the frequency of

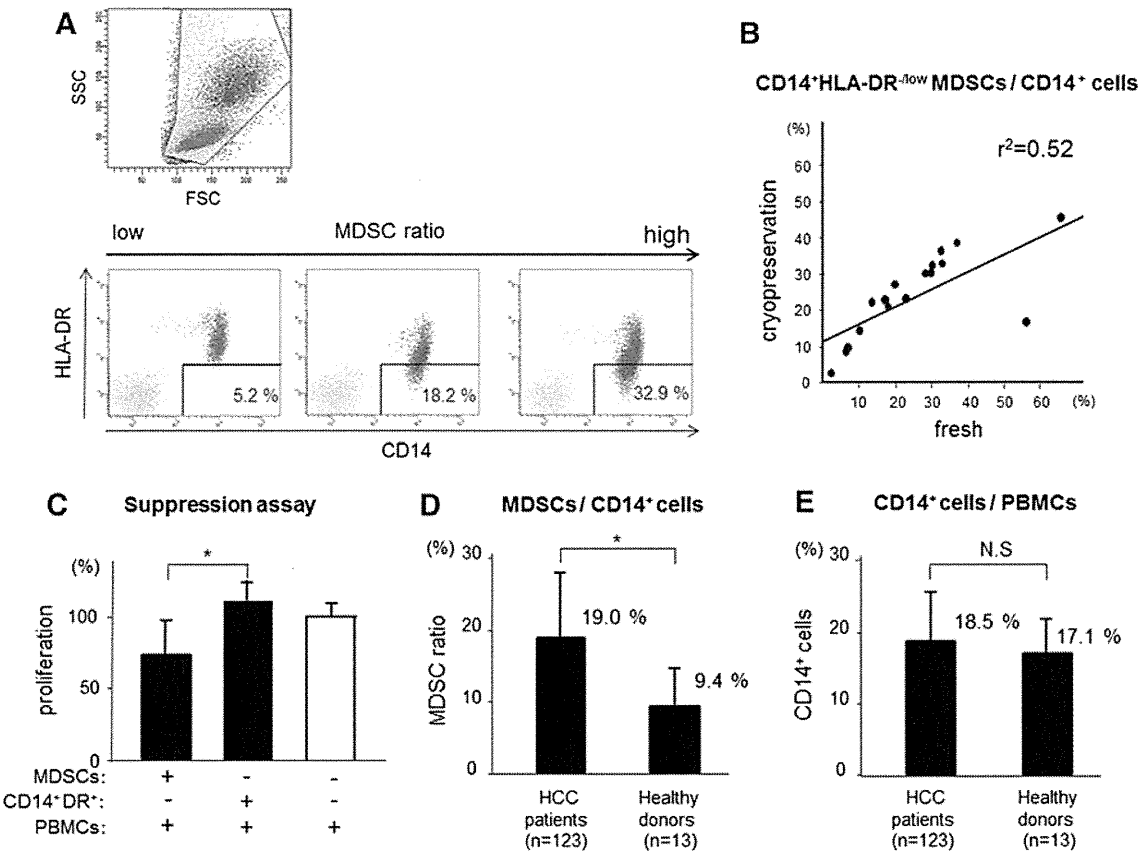

Fig. 1 **a** Flow cytometry shows $CD14^{+}HLA\text{-}DR^{-/low+}$ MDSCs. PBMCs from patients and healthy donors were labeled with anti-CD14 and HLA-DR. Three staining examples of HCC patients are shown in the order from a small number (*left*) to a large number (*right*). **b** The increase in $CD14^{+}HLA\text{-}DR^{-/low}$ MDSCs/$CD14^{+}$ cells in cryopreserved PBMC correlated with that in fresh PBMC ($r^2 = 0.52$). **c** Proliferation of PBMCs stimulated by anti-CD3/28 in the presence or absence of MDSCs was measured by ^{3}Hincorporation assay. $CD14^{+}HLA\text{-}DR^{-/low}$ MDSCs significantly decreased autologous PBMC proliferation ($n = 4$; *, $p < 0.05$). **d** The frequency of MDSCs was significantly higher in HCC patients than healthy donors (*, $p < 0.01$). **e** Overall frequencies of $CD14^{+}$ cells did not differ significantly

$CD15^{+}CD14^{-}CD11b^{+}CD33^{+}$ cells in HCC patients was higher than that in healthy donors (2.84 vs. 2.06 %, $p = 0.073$) (Suppl. figure 1B). The frequency was correlated with the stage of HCC (stage III and IV: 3.69 % ($n = 13$) vs. stage I and II: 2.39 % ($n = 24$), $p = 0.022$) (Suppl. figure 1C).

Relationship between the frequency of Tregs and MDSCs

It is well known that the frequency of circulating Tregs is increased and correlated with disease progression in HCC patients. The frequency of $CD4^{+}$ $CD25^{+}$ $CD127^{-/low}$ Tregs was significantly increased in HCC patients (Suppl. figure 2A) and associated with tumor progression (Suppl. figure 2B). However, there was not a strong correlation between the frequency of MDSCs and Tregs in our study (Suppl. figure 2C).

Identification of host factors related to the frequency of MDSCs in HCC patients

We divided the HCC patients into two groups using the threshold of an MDSC ratio of 22 %. This threshold is the average +2SD of the MDSC ratio in non-HCC patients. In the group with high frequency, the tumor factors including size, multiplicity, and stage were significantly worse (tumor size, 28.3 vs. 24.4 mm; tumor multiplicity (multiple/solitary), 27/12 vs. 42/42; TNM stage (I and II vs. III and IV), 17/22 vs. 60/24, $p < 0.05$) (Table 1). Moreover, hepatic reserve was also worse in the group with high frequency (Child-Pugh classification (A/B/C), 20/17/2 vs. 64/16/4, $p < 0.05$). In addition, overall survival was significantly shortened in the group with high frequency (hazard ratio 2.67, $p = 0.008$) (Suppl. figure 3A), and recurrence-free survival was also significantly shortened (hazard ratio 1.94, $p = 0.010$) (Suppl. figure 3B).

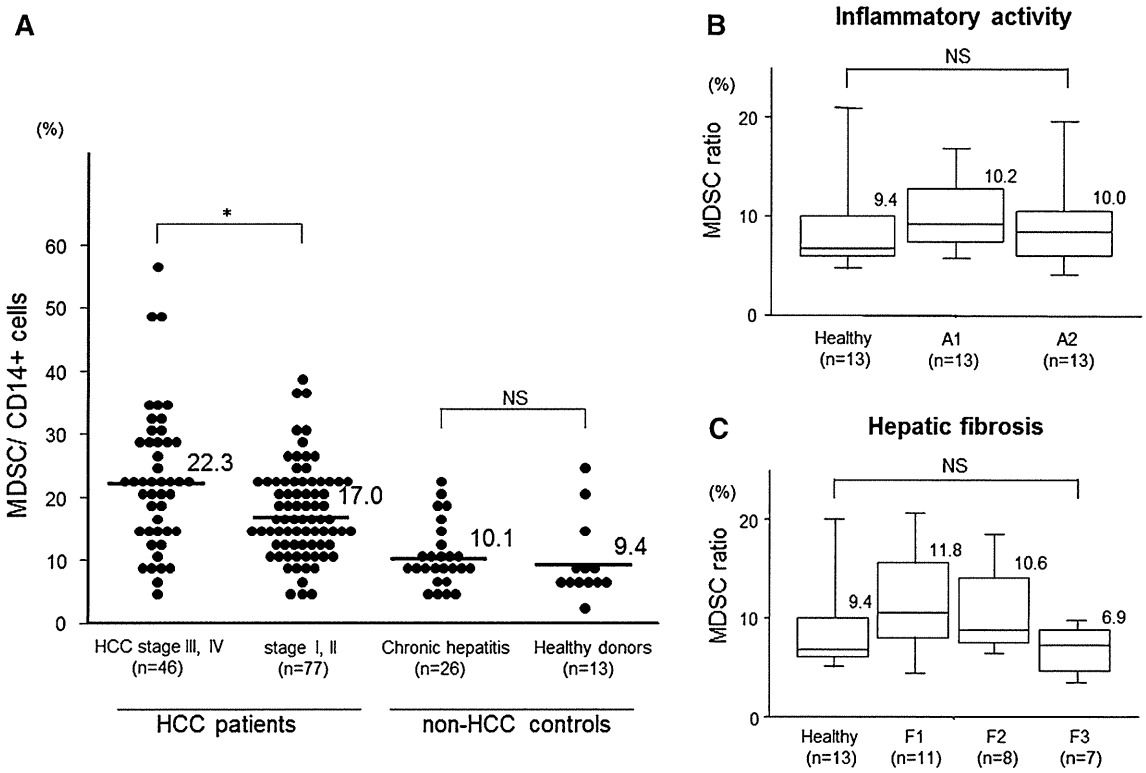

Fig. 2 **a** Scatter plots of MDSC ratio ($CD14^+HLA\text{-}DR^{-/low}$ MDSCs/ $CD14^+$ cells) in patients and healthy donors. The frequency of MDSCs was significantly increased in HCC patients compared with that in non-HCC controls. Moreover, the frequency of MDSCs was correlated with tumor progression (stage III and IV: 22.3 % ($n = 46$) vs. stage I and II: 17.0 % ($n = 77$); *, $p < 0.05$). In non-HCC controls, there was no significant difference in the frequency of MDSCs. **b**, **c** In non-HCC patients, the frequency of MDSCs did not change depending on the degree of fibrosis or inflammatory activity of the liver according to the Metavir scoring system

Relationship between serum cytokine levels and the frequency of MDSCs

In previous studies, the balance of circulating cytokines was thought to promote accumulation and activation of MDSCs [18, 31–34]. Therefore, we examined the relationship between serum cytokine levels and the frequency of MDSCs in HCC patients. In 54 HCC patients, serum levels of cytokines and chemokines were measured using the Bio-Plex Protein Array system. Serum concentrations of IL-10, IL-13, and VEGF were significantly increased in the group with a high frequency of MDSCs (Table 2). In addition, there was a positive correlation between these cytokine levels in serum and the frequency of MDSCs. We also examined the relationship between serum cytokine levels and the frequency of Tregs. We divided the HCC patients into two groups using the threshold of 7 %, which is the average +2SD of the % of Tregs among $CD4^+$ cells in non-HCC patients. Serum concentration of IL-10 was significantly increased in the group with a high frequency of Tregs (Suppl. table 2).

Kinetics of MDSCs before and after curative RFA therapy

We examined the frequency of MDSCs before and after curative RFA therapy in 33 patients. For this analysis, blood samples were obtained on the day of treatment (before) and 2–4 weeks after treatment (after). The frequency of MDSCs was significantly decreased after RFA therapy (18.0 to 15.5 %, $p < 0.05$) (Fig. 3a). However, in several patients, the frequency of MDSCs remained at a high level compared with that in non-HCC patients. The clinical parameters before RFA were not statistically different between the patients with and without a high frequency of MDSCs after RFA (Suppl. table 3).

Next, we followed up these patients for recurrence and analyzed the risk factors. If a high frequency of MDSC was observed after curative RFA therapy, the recurrence-free survival was significantly shortened (Fig. 3b). In contrast, the frequency of MDSCs before treatment did not affect the recurrence. In univariate analysis for recurrence, post-treatment MDSC ratio ≥22 % ($p = 0.023$) and tumor